



Research Article

Statistical investigation of the effects of different origin aggregate properties on the mechanical properties of concrete

Ahmet Teymen ¹, *

¹ Department of Mining Engineering, Niğde Ömer Halisdemir University, TR (Türkiye), ateymen@ohu.edu.tr

*Correspondence: ateymen@ohu.edu.tr

Received: 15.12.2022; **Accepted:** 30.07.2023; **Published:** 31.08.2023

Citation: Teymen, A. (2023). Statistical investigation of the effects of different origin aggregate properties on the mechanical properties of concrete. *Revista de la Construcción. Journal of Construction*, 22(2), 482-508. <https://doi.org/10.7764/RDLC.22.2.482>.

Abstract: Aggregates are one of the most important components of the concrete mix and the aggregate properties have a great influence on the properties of the hardened concrete. From this point of view, the contribution of the nature of the aggregate to the general mechanical behavior of concrete should be better understood and investigated. The main purpose of this study is to present practical and useful equations for the rapid evaluation of the basic properties of concrete, especially during the preliminary design phase. A series of laboratory studies were conducted to determine the effects of twenty aggregates with very different origins and properties on various properties of concretes. Laboratory tests with the same or similar principles as aggregate rocks have been repeated for concrete samples produced using these aggregates.

Nine SRA equations were generated to directly predict similar concrete properties with the help of aggregate properties. Equations with very high coefficients of determination were produced between various aggregate properties and concrete properties except for the SHH property. In addition, nonlinear multiple regression analysis (NMRA) was used for twenty-four equations to predict some basic properties of concrete (strength, abrasion, tensile, and impact). The performances of the derived equations were evaluated with a statistical tool developed by the author. Accordingly, the models with the strongest prediction capacity were obtained for STS_C, LA_C, CS_C, and, IE_C respectively. Results from NMRA showed that equations with the highest coefficient of determination were obtained with Model-3 for CS_C (Equation 15), and STS_C (Equation 18), and Model-1 for LA_C (Equation 22), and IE_C (Equation 31).

Concrete has a complex structure that is affected by many parameters. In accordance with this complex nature, the approach to predict the main concrete properties with nonlinear multiple methods by including similar aggregate properties as well as non-destructive methods representing concrete/aggregate (hardness, ultrasonic pulse velocity and physical properties) has been successful. The extremely high coefficients of determination, ranging from 0.81 to 0.96, obtained with NMRA, indicate that basic concrete properties can be strongly predicted by aggregate properties and some concrete properties that can be tested non-destructively.

Keywords: concrete properties, aggregate type, impact energy, abrasion resistance, nonlinear multiple regression.

Abbreviations

NMRA	Nonlinear multiple regression analysis
CS _C	Compressive strength of concrete
CS _R	Compressive strength of rock
E _C	Elastic modulus of concrete
STS _C	Splitting tensile strength of concrete
BTS _R	Brazilian tensile strength of rock
LA _C	Los Angeles abrasion of concrete
LA _R	Los Angeles abrasion of rock
IE _C	Impact energy of concrete
IE _{R-RIHN}	Impact energy of rock
SHH _C	Schmidt hammer hardness of concrete
SHH _R	Schmidt hammer hardness of rock
FTS _C	Flexural tensile strength of concrete
PLI _C	Point load index of concrete
PLI _R	Point load index of rock
UPV _C	Ultrasonic pulse velocity of concrete
UPV _R	Ultrasonic pulse velocity of rock
UW _C	Unit weight of concrete
UW _R	Unit weight of rock
WA _C	Water absorption of concrete
WA _R	Water absorption of rock
P _{gC}	Apparent porosity of concrete
P _{gR}	Apparent porosity of rock
w/c	Water/cement ratio
ACV	Aggregate crushing value
AIV	Aggregate impact value
RIHN	Rock impact hardness number
XRF	X-ray fluorescence method
XRD	X-ray diffraction method
WMAPE	The weighted mean absolute percentage error
VAF	Variance account factor
RMSE	Root mean squared error
RSR	Root mean square error to observation's standard deviation ratio
R ²	Maximum determination coefficient value
PI _{at}	Performance index value created by the author
ITZ	Interfacial transition zone

1. Introduction

Concrete, which is one of the most widely used materials in the construction industry due to its many properties, especially high compressive strength, ranks second after water in the world's most consumed material ranking (Balaji et al, 2017). At the end of the first decade of the 21st century, more than 4 billion tons of cement are used annually which indicates that about 15 billion cubic meters of concrete are produced in the World (statistica.com). Aggregate constitutes almost 75-80% of the concrete volume and is the most basic component of concrete (Neville, 1995). This high ratio indicates that aggregate properties play a very important role in concrete properties (ACI, 2001). It is possible to produce concretes with different properties by keeping the cement quality constant and using aggregates with different physico-mechanical features (Neville, 1981). The most important mechanical property of load-bearing concrete is considered CS_C. For this reason, the relationship between composition and CS_C has been for a long time research topic for researchers.

The important parameters that most affect the strength of hardened concrete are types of coarse aggregate, the amount and types of cement, w/c, additives, and curing conditions (Aitcin & Mehda, 1990; Ezeldin & Aitcin, 1991; Zhou, Lydon, & Barr, 1995; de Larrard & Belloc, 1997; Özturan & Çeçen, 1997; Wu et al., 2001; Mannan et al., 2002; Beshr, Almusallam & Maslehuddin, 2003; Chi et al., 2003; Kılıç et al., 2008; Aminur et al., 2010; Meddah, Zitouni & Belâabes, 2010; Ahmad & Alghamdi, 2012; Uysal, 2012; Abdullahi, 2012; Kılıç & Sertabipoğlu, 2015; Vishalakshi, Revathi & Reddy, 2018; Kılıç et al., 2019; Góra & Piasta, 2020; Tunc & Alyamac, 2020; Karaman & Bakhytzhn, 2020; Góra & Szafraniec, 2020; Wu et al., 2020; Dong et al., 2022).

In the literature, there are some studies about the effects of coarse aggregate types and their origins on the strength of the concretes. They reported that the CS_C of concrete is controlled by the specifics of the interface between cement and aggregate, cement paste, and coarse aggregate. Additionally, for the same quality paste, different types of aggregate with different mineralogy, textures, shapes, and strengths result in various concrete strengths. The weaker aggregates reduce the strength of concrete. Coarse aggregate strength and low w/c are extremely necessary and important for high-strength concrete production. Aitcin & Mehda, 1990 conducted a laboratory study that examined the influence of four coarse-aggregate types (Northern California) on the elastic behavior and CS_C of very high-strength concretes. Their results show that concretes with diabase and limestone aggregates have higher E_C and CS_C than concretes with granite and river gravel. The authors declare that this difference in strength is due to mineralogical differences in the aggregate types. Zhou, Lydon, & Barr, 1995 used six different aggregates to produce high-strength concrete with a low w/c. They measured the E_C of the produced concrete at 7, 28, and 91 days of curing. They stated that, except for aggregates with very high and low elasticity, the concrete modulus can be predicted quite well in 28 days with well-known models. de Larrard & Belloc, 1997 conducted a comprehensive theoretical study on the effect of aggregates (5 sources of aggregate) on the CS_C (13 mixtures). They produced some equations about maximum paste thickness and its effect on CS_C . The average distance between two adjacent coarse aggregates is defined as the maximum paste thickness. The second type of effect is relevant the bond effect and ceiling effect. The three effects of aggregate on CS_C gave an accuracy of close to 2.2 MPa for these mixes. Özturan & Çeçen, 1997 produced concrete of different strength levels and investigated the effect of coarse aggregate type on CS_C , FTS_C , and STS_C . They determined that gravel concrete had the lowest CS_C and basalt concrete had the highest CS_C . According to their results, the improvement in the strength of cement paste provides about a 30 percent increase in FTS_C and STS_C when the CS_C is not affected. They also stated that FTS_C in high-strength concretes is mostly affected by the strength of the paste and the surface characteristics of the coarse aggregate. According to the results, CS_C is mainly controlled by the coarse aggregate type.

Wu et al., 2001 examined the effect of coarse aggregate type on some concrete properties in concrete poured with aggregates produced from rocks such as granite, quartzite, marble, and limestone. They determined that stiffness, strength, and fracture energy for high-strength concrete depend on the aggregate type. The w/c ratio of high-strength concrete is generally less than 0.4 and the strength of the paste and the bond at the interface may be similar to the strength of the coarse aggregate. Beshr, Almusallam & Maslehuddin, 2003 investigated the effects of coarse aggregates on the properties (CS_C , E_C , and FTS_C) of four different concrete. According to the results of this study, the lowest CS_C was obtained with limestone and the highest CS_C was obtained with steel slag aggregates. Kılıç et al., 2008 examined the effect of the type of coarse aggregate on the abrasion resistance, FTS_C , and CS_C of concrete. They used five different aggregates (sandstone, quartzite, basalt, gabbro, and limestone). The results of the study using five different aggregates showed that aggregate strength and rock texture significantly affected the concrete strength. Ćosić et al., 2015 investigated the aggregate types (dolomite or steel slag) and aggregate size (4–8 mm and 8–16 mm) on the properties of pervious concrete with X-ray tomography.

Bentz et al. 2017, conducted a series of laboratory studies to examine the effect of aggregate type on concrete performance and to identify the aggregate properties that have the greatest impact on this performance. They investigated the hardened properties such as compressive, splitting tensile and flexural strengths and electrical resistivity of concrete samples made with different coarse aggregate types such as diabase, dolomite, dolomitic limestone, highly absorbent limestone, micritic limestone, granite, granitic gneiss, siliceous gravel, marble, meta-basalt, quartz and sandstone. Their results showed that the choice of coarse aggregate for similar mixing ratios can have a measurable effect on concrete performance in terms of both mechanical and electrical resistance properties. Alqarni et al., 2020 experimentally investigated the effects of coarse aggregate properties (limestone, quartzite, scoria, and steel slag aggregate) on the shear behavior of reinforced concrete thin beams. According to their results, they observed a higher ultimate shear strength in concretes produced with aggregates with high abrasion resistance. They noted that for beams cast with similar compressive strength categories, the normalized shear strength generally followed an increasing trend with aggregate abrasion resistance and aggregate density. Góra & Piasta, 2020 produced twenty-four different concretes with thirteen different aggregates produced from rocks (basalt, granite, granodiorite, dolomite, quartzite, gravel) from various mines in Ukraine and Poland. They examined the relationships between ACV and concrete's mechanical properties (CS_C , STS_C , and E_C). They determined that the strongest associations with ACV were between E_C , STS_C , and CS_C , respectively. Karaman & Bakhytzhan, 2020 applied CS_C , PLI_C , and UPV_C tests to the concrete they produced with eight different aggregates. They applied the CS_R , PLI_R , UPV_R , Pg_R , UW_R , and AIV tests to the aggregates and intact

rocks. They found that PLI_C , UPV_C , CS_R , PLI_R , and UPV_R were statistically significant independent variables in estimating CS_C . Tunc & Alyamac, 2020 tried to determine the relationship between LA_R and CS_C , taking into account the aggregate-cement and w/c. They prepared concrete mixtures with different aggregate types and different w/c ratios. They developed two new models with the optimization method they performed with Response Surface Methodology. With the help of these models, they determined that the STS_C and CS_C can be calculated with high accuracy by using LA_R , w/c, and aggregate/cement ratio for different mix designs. Yehia et al., 2020 used two sizes of natural aggregate and two sources of lightweight and recycled aggregates to investigate the effect of aggregate type and sample size and shape on the compressive strength of concrete. The results showed that the concrete compressive strength and modulus of elasticity were significantly affected by the aggregate type. The flexural strength and the split tensile strength were less affected by the aggregate type, which was also confirmed by the values estimated by the ACI equations.

Hansen et al. in their study, published in 2021, aimed to clarify the relative effects of aggregate mineralogy and shape on the fundamental relationships between concrete's mechanical properties. They found that mineralogy and shape had a significant effect on the relationships between compressive strength, elastic modulus, and splitting tensile strength. They used these datasets to compare various empirical relationships found in the literature to determine their ability to predict elastic modulus and elastic modulus based on compressive strength. Mousavi & Ranjbar, 2021 investigated the fracture properties of high-strength concrete using 150 beams they produced with a total of 10 mixing designs with different amounts of silica fume and various aggregates. In one of the research results, they revealed that the aggregate type significantly affects the fracture and mechanical parameters. They noted that quartzite and andesite aggregates increased fracture energy and characteristic length compared to limestone aggregate.

Naderi & Kaboudan, 2021 studied the influence of aggregate type on the strength and permeability of concrete and found that aggregate type had a significant impact on the compressive strength and permeability of concrete, while the geometric shape of the aggregate had little influence on the compressive strength and permeability of concrete. Wang et al., 2021 produced concrete under the same conditions, using aggregates made from different rocks such as diabase, basalt, limestone, and gneiss. They performed tests such as slump flow, flexural strength, compressive strength, shrinkage rate, chloride penetration resistance and freeze-thaw resistance of these produced concretes. In this study, they revealed the effects of aggregate type on the concrete properties listed above. Patowary & Al Mahmood, 2022 report the results of an experimental study examining the effects of six different natural coarse aggregate types on the mechanical properties of concrete. In this study, they aimed to find the best locally available natural coarse aggregate for concrete preparation in terms of mechanical strength. They examined compressive strength, splitting tensile strength, and modulus of elasticity at 7, 14, and 28 days of curing age. Mostofinejad et al., 2023 conducted an experimental study to develop empirical models to predict the mechanical properties of high-strength concrete, including the combined effects of silica fume, coarse aggregate type, water-cement ratio, and curing time. They prepared 45 different concrete mixes using five different ratios of silica fume, three different water-cement ratios, and three different aggregates. The results showed that the mixture with a water-cement ratio of 0.24, with 15% silica fume substitute and quartzite aggregate, gave the highest tensile, flexural, and compressive strength.

This research reports laboratory tests and statistical analyzes to see the effects of aggregates with very different physical and mechanical properties (CS_R , LA_R , BTS_R , IE_{R-RIHN} , UPV_R , SHH_R , UW_R , Pg_R , and WA_R) on the different properties of the concretes. In addition, laboratory tests with the same or similar principles as aggregate rocks have been repeated for concrete samples produced using these aggregates. In this way, it has been tried to estimate similar concrete properties with the aid of aggregate properties. Experiments conducted for concrete samples were as follows (CS_C , LA_C , STS_C , IE_C , UPV_C , SHH_C , UW_C , Pg_C , and WA_C). For this purpose, aggregates were produced by using twenty rocks having different strengths, textures, and origins, and these aggregates were graded to have the same size distribution and used in concrete production. Firstly, according to the test results, the relations between the similar concrete and aggregate properties mentioned above were determined. Then, the relationship between concrete strength and all aggregate and concrete properties was evaluated and the results were explained in detail. Figure 1 summarizes the methodology followed during the conduct of this study.

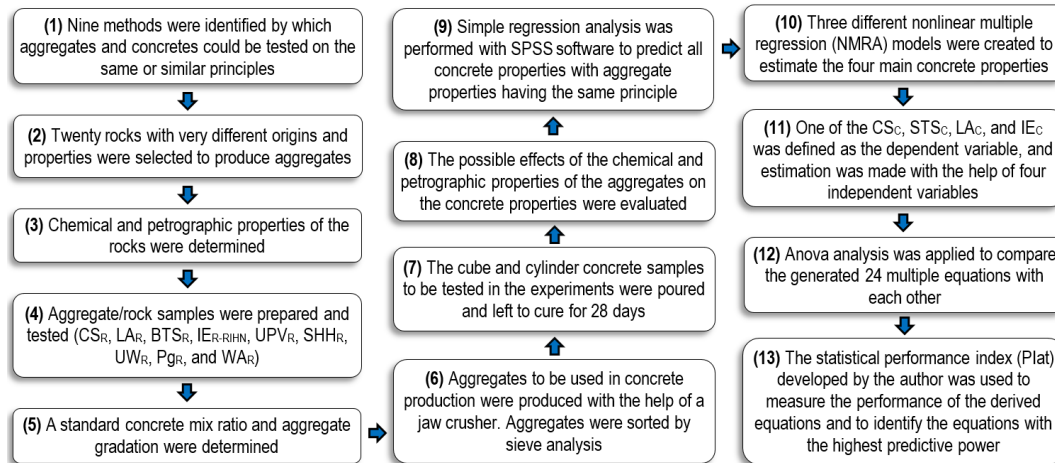


Figure 1. The methodology followed in this study.

The effects of coarse aggregate properties on concrete strength is a well-known issue that has been discussed many times in the literature. Most of the researchers focused on maximum aggregate size, aggregate particle distribution, aggregate shape, and aggregate chemical content. In addition, most of these studies were carried out using a limited number of aggregates. In this study, twenty different aggregates were produced using a large number of rocks from different geological origins. The use of a large number of aggregates with a very wide strength range in the same study allowed examining the effects of coarse aggregate on concrete strength in more detail in terms of aggregate. In addition, the relationships between the hardened concrete properties and the similar/same properties of the aggregates used in the production of these concrete were statistically examined in terms of nine different parameters. In this respect, the study also contributes to the limited literature. In this study, nonlinear multiple regression models are presented, in which the most basic properties of concrete (strength, abrasion, tensile, and impact) can be reliably predicted by practical and non-destructive test methods. The strongest aspect of the study is that the test methods that make up the independent variables in these models can be applied without damaging the samples by using samples prepared for the compressive strength of rock or concrete.

The biggest handicap in this study is that crushed stone sand produced from aggregates was preferred instead of river sand in concrete mixtures. This situation caused an increase in the w/c ratio and a relative decrease in the effect of coarse aggregate on concrete properties. It is very clear that with similar studies that can be carried out considering this problem, it is possible to reach outputs that will make important contributions to the literature.

2. Materials and mixture design

2.1. Materials

Aggregate rocks used in the production of concretes were collected from natural outcrops, quarries, and natural stone plants in different regions of Turkey. Aggregates used for this study were selected from 93 rocks in the article published by Teymen & Mengüç, 2020. Twenty types of aggregates were produced from these rocks: plutonic (six), volcanic (four), pyroclastic (two), metamorphic (one), and sedimentary (seven). Although the use of a few of the selected aggregates (tuff, gypsum, claystone, etc.) in concrete is not common/appropriate, the main criterion for the selection of aggregates is the strength properties of aggregates. The rules recommended by TS 706 EN 12620+A1, 2009 have been taken into consideration in the preparation of the aggregates and the application of the tests. The main rock pieces were first crushed by a laboratory-type jaw crusher and then it was sieved and separated into three different sizes of -16+8 mm (-16+11.2mm and -11.2+8 mm) as coarse aggregate, -8+4 mm as medium aggregate, -4+2 mm as fine aggregate and -2 mm crushed stone sand (-2+1mm, -1+0.5mm, -0.5+0.25, -0.25+0.15, -0.15+0.063 and -0.063mm). In Figure 2, cross-sectional views of the hardened concrete produced by using twenty different aggregates obtained by the cutting-polishing process and the coarse aggregate samples produced by breaking the bedrock in a jaw crusher are shown.

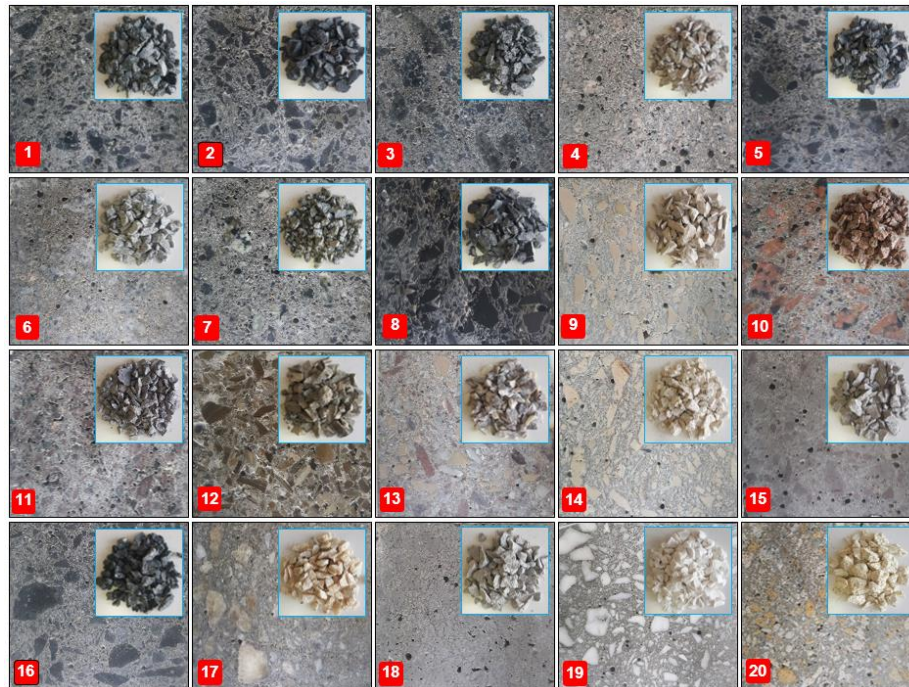


Figure 2. Images of hardened concrete surfaces cut with circular saw and aggregates used in concrete production.

When determining the separated aggregate combinations, a grading following the requirements of TS 706 EN 12620+A1, 2009 was used. All aggregates were prepared at the same grain-size distributions to eliminate the influence of the aggregate size on the concrete properties. The aggregate gradations prepared to remain within the standard limits are given in Figure 3. In preparation for concrete mixtures, CEM I 42.5 R type normal Portland cement complying with relevant TS EN 197-1, 2004 was used. Portland cement was procured from the Niğde cement plant (CIMSAs). 28 days C_{sc} , specific gravity of cement, and blain specific surface area of cement is 48.1 MPa, 3.06 g/cm³, and 3641 cm²/g, respectively. The initial and final setting time of the cement is 190 and 260 minutes, respectively. Table 1 shows the chemical compositions of the cement and aggregate materials used in the study, determined by the XRF. Glenium 51 which is a modified polycarboxylic ether polymer used as water reduction in concrete mixtures was obtained from BASF-The Chemical Company in Turkey. The desired reduction of the slump (80±20 mm) was achieved with Glenium 51 (TS EN 934-2, 2011).

Table 1. Chemical composition of the cement and aggregates (XRF results)

Oxide (%)	M ₁	M ₂	M ₃	M ₄	M ₅	M ₆	M ₇	M ₈	M ₉	M ₁₀	M ₁₁	M ₁₂	M ₁₃	M ₁₄	M ₁₅	M ₁₆	M ₁₇	M ₁₈	M ₁₉	M ₂₀
SiO ₂	43.7	59.8	51.2	65.9	60.7	70.6	55.6	4.18	2.13	74.9	63.3	24.1	2.46	0.31	65.6	47.4	0.22	73.4	0.20	71.2
Al ₂ O ₃	9.40	16.7	17.5	16.6	14.7	14.2	17.0	1.20	0.73	14.2	14.8	4.97	1.70	0.23	17.2	-	0.22	14.8	0.10	15.8
Fe ₂ O ₃	13.5	8.62	12.0	3.79	7.74	3.48	7.88	1.23	0.65	2.47	6.13	3.66	1.69	0.21	6.01	16.5	0.66	2.29	-	4.85
CaO	22.1	10.3	12.4	4.07	12.7	4.47	3.57	91.8	81.7	1.44	10.0	51.2	92.9	98.5	5.62	1.05	97.7	1.58	29.7	2.96
MgO	5.80	0.87	3.50	-	-	-	-	0.72	12.2	-	-	9.0	0.72	0.48	-	32.1	0.85	-	3.65	-
SO ₃	1.70	-	-	-	0.14	0.20	2.50	0.38	0.30	-	0.23	3.94	0.04	0.08	0.12	0.34	0.14	0.10	46.0	-
K ₂ O	1.43	3.38	2.94	8.11	2.17	5.09	5.54	0.33	0.22	6.50	2.72	2.74	0.41	0.02	3.63	0.09	0.02	4.47	-	4.15
Na ₂ O	-	-	-	-	-	-	2.00	-	2.00	-	1.50	-	-	-	-	-	-	2.60	0.10	-
TiO ₂	0.60	-	-	0.53	0.74	0.45	1.05	-	-	0.19	0.69	-	-	-	0.80	-	-	0.36	-	0.55
MnO	0.20	0.14	0.21	0.09	0.12	0.07	0.36	0.08	0.03	0.07	0.10	0.2	0.03	0.01	0.10	0.20	0.15	0.06	-	0.08
ZrO ₂	-	-	-	0.24	-	-	0.78	-	-	-	-	-	-	-	0.17	-	-	-	-	-
BaO	0.16	-	-	0.18	0.14	0.16	0.39	-	-	0.13	0.14	-	-	-	0.22	-	-	0.12	-	0.15
ZnO	0.03	-	0.02	0.03	0.07	0.21	1.56	0.01	0.03	0.02	-	0.03	0.01	0.01	0.01	0.29	0.01	0.01	-	0.01
NiO	0.01	0.01	0.01	-	-	-	-	-	-	-	-	0.02	-	0.01	-	0.63	-	-	-	-
PbO	-	-	-	-	-	0.09	0.54	-	-	-	-	-	-	-	-	0.21	-	-	-	-
MoO ₃	-	-	-	-	-	0.65	1.02	-	-	-	-	-	-	-	-	0.50	-	-	-	-

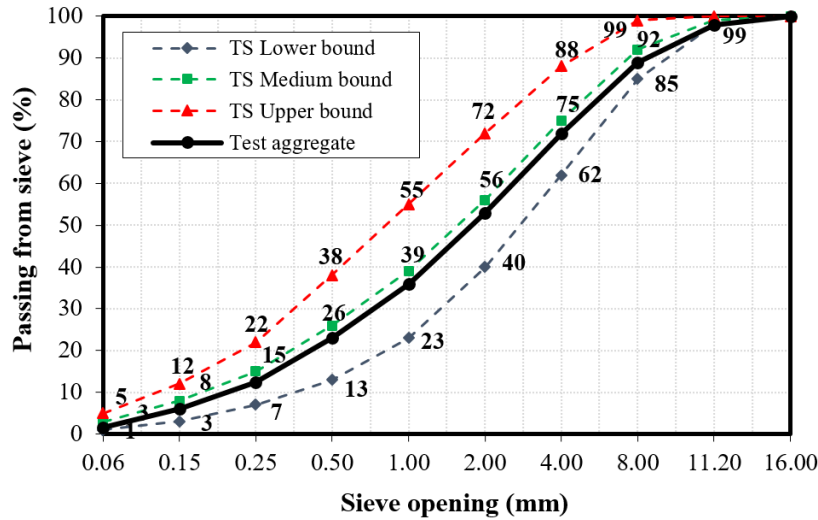


Figure 3. Total used aggregate grading with standard limits (TS 706 EN 12620+A1, 2009).

2.2. Mixture design

The correct comparison of twenty concrete mixtures produced with very different aggregates depends on their production with the same principle. From this point of view, the design was created in such a way that approximately 61.5% of the total volume is aggregate, 23% is water, 13.5% is cement, 2% is air and 0.4% is superplasticizer. The unit weight values of the aggregates used in the experimental study differ due to their different geological origins (varying between 1.52 and 2.96). The amount of aggregate in the mixtures was calculated based on the unit weight of the aggregate rocks. Therefore, the aggregate amounts for each sieve size are the same in volume (coarse aggregate %8, medium aggregate %17, fine aggregate %19, and crushed stone-sand %56). Due to the effect of aggregates of different origins on workability, w/c ratios were tried to be kept constant around 0.55. 1.15 percent by mass of cement in concrete mixtures were used as superplasticizers. The aggregates used were surface dry conditions. A pan mixer was used to obtain a homogeneous concrete mixture, and for each type of mixture, cylindrical molds of 100 mm diameter and 200 mm length and cube molds of 100 mm side length were used. Concrete samples using a vibrator for compaction were removed from the molds the next day after casting and cured in laboratory conditions for 28 days. The fresh unit weights of the prepared concrete mixtures, the unit weights at the end of the 28-day curing period, and the unit weight values of the aggregate rocks are given in Figure 4 comparatively.

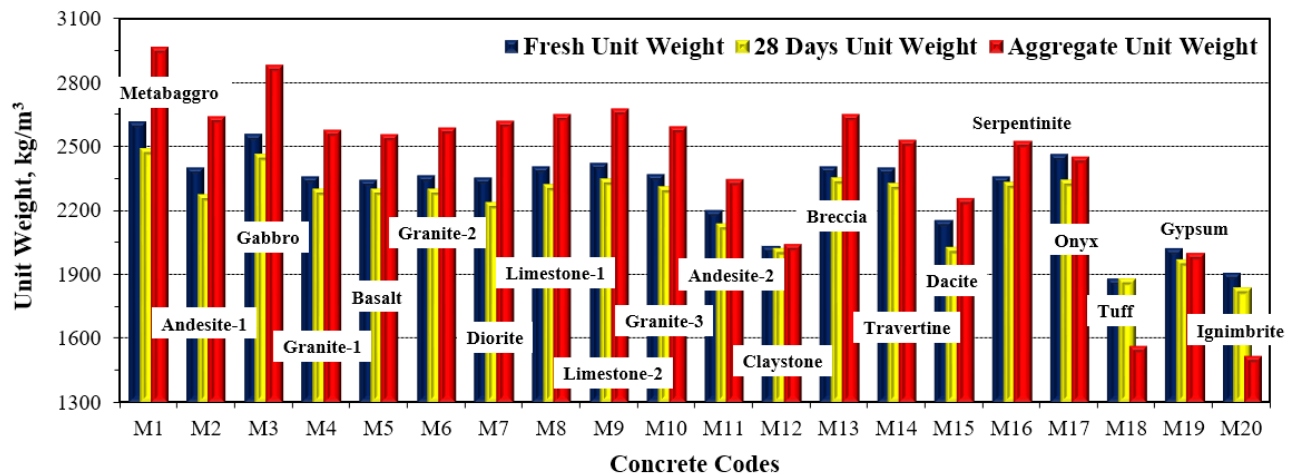


Figure 4. Column chart showing unit weights of concrete mixes and aggregate rocks.

3. Experimental study

To investigate the effect of aggregate stones on concrete properties (especially strength) some mechanical and physical features of the corresponding rocks were tested. During the preparation and testing of the produced aggregate stones, the rules and procedures given in the ISRM, 2007 were generally followed. In this context, properties of the aggregate rocks; CS_R , BTS_R , LA_R , SHH_R , UPV_R , IE_{R-RIHN} , UW_R , WA_R , and Pg_R were determined. After 28 days of standard curing, CS_C , $STSC$, LA_C , SHH_C , UPV_C , IE_C , UW_C , WA_C , and Pg_C tests were performed on concrete specimens. Experimental results were given in Table 2 and Table 3.

Table 2. Average test results of aggregate rocks.

Code	Rock Type	Rock Class	Rock/Aggregate Properties									
			CS_R MPa	BTS_R MPa	LA_R %	SHH_R rebound	UPV_R km/sec	IE_{R-RIHN} *	UW_R g/cm ³	WA_R %	Pg_R %	
M1	Gabbro 1	Plutonic	232.7	16.0	19.4	60.2	5.82	1.05	2.96	0.25	0.73	
M2	Andesite 1	Volcanic	207.0	14.9	16.9	52.9	5.97	0.85	2.64	0.13	0.33	
M3	Gabbro 2	Plutonic	191.8	16.3	16.9	54.0	6.33	1.05	2.88	0.07	0.21	
M4	Granite 1	Plutonic	137.8	11.8	20.1	51.0	4.84	0.71	2.58	0.47	1.21	
M5	Basalt	Volcanic	135.5	12.4	16.9	57.3	5.03	0.83	2.56	0.62	1.58	
M6	Granite 2	Plutonic	110.6	9.9	32.1	54.2	5.08	0.65	2.59	0.38	0.99	
M7	Diorite	Plutonic	109.2	8.1	26.0	53.7	5.21	0.60	2.62	0.17	0.45	
M8	Limestone 1	Sedimentary	108.4	6.6	28.5	57.6	5.95	0.61	2.65	0.29	0.23	
M9	Limestone 2	Sedimentary	106.8	8.9	26.1	48.2	6.57	0.61	2.67	0.18	0.23	
M10	Granite 3	Plutonic	106.2	10.6	29.4	60.4	4.95	0.53	2.59	0.19	0.49	
M11	Andesite 2	Volcanic	95.6	7.0	37.6	53.4	3.45	0.40	2.35	2.73	6.50	
M12	Claystone	Sedimentary	79.3	8.4	32.1	35.4	3.02	0.47	2.05	3.19	5.97	
M13	Breccia	Sedimentary	78.3	7.9	27.1	51.1	5.93	0.51	2.65	0.05	0.15	
M14	Travertine	Sedimentary	77.3	8.7	30.1	49.8	5.30	0.49	2.53	1.14	2.89	
M15	Dacite	Volcanic	65.1	5.0	30.7	40.8	3.23	0.48	2.26	5.66	12.74	
M16	Serpentinite	Metamorphic	34.4	2.4	34.1	37.2	3.66	0.33	2.53	0.87	2.01	
M17	Onyx	Sedimentary	21.6	3.0	55.1	41.0	3.12	0.11	2.45	1.01	1.85	
M18	Tuff	Pyroclastic	19.4	1.7	58.9	31.5	1.55	0.16	1.57	17.97	28.14	
M19	Gypsum	Sedimentary	14.0	1.7	62.1	20.0	2.02	0.18	2.00	13.49	16.12	
M20	Igimbrite	Pyroclastic	6.7	1.3	59.3	22.8	1.25	0.05	1.52	20.81	31.65	

While the guidelines in TS EN 12504-4, 2012 were followed for UPV tests of concrete (Figure 5f), UPV tests of rocks were carried out by considering the principles in ISRM, 2007. The compressional P wave velocities of concrete and rock (Cylinder samples for CS) were measured using the high-frequency ultrasonic pulse technique. The transmitter was positioned on a plane opposite that upon which the receiver was placed. The liquid coupling gel was applied on the surface of the samples for good acoustic contact. The transducers were energized from the pundit instrument and the travel time of P waves was noted for each sample. P wave velocities of all samples were calculated from the measured travel time and length of samples.

The Schmidt hammer hardness method is routinely used to test the quality and strength of concrete and rock (Figure 5e). There is a strong relation between SHH value and compressive strength values. The tests were carried out on the flat surfaces of the rock blocks using an N-type Schmidt hammer. ISRM, 2007 suggested method was followed in the tests. As described in the standard, 20 rebounds were taken from the rock or concrete surface and the average of the highest 10 values was calculated. The averaged Schmidt rebound values were corrected based on a correction factor.

The impact resistance of the concrete specimens was tested at the end of 28 day curing period by using the drop weight procedure recommended by ACI Committee 544.2R-89, 2009. The disc samples used for the test have a diameter of 100 mm and a thickness of 64 mm. The disc specimens were cut from 100 mm diameter x 150 mm length cylinder concretes using a stone cutter. The impact test was performed by dropping a hammer (4.54 kg) from a height of 457 mm repeatedly on a 64 mm diameter hardened steel ball. The position of the steel ball placed on the concrete samples and the failure pattern of the disc specimens after ultimate failure are shown in Figure 5a. The number of blows required to cause the ultimate failure was recorded as the ultimate failure strength. The impact energy delivered to the concrete sample was calculated by the equation

given in brackets ($E = N.m.g.h$). Where E: impact energy (J=N.m), m: the mass of drop hammer (kg), g: gravity acceleration ($9.81m/s^2$), h: height of drop hammer (m), N: number of blows. In this study, if the concrete samples split up completely into halves before touching the lugs, then this was accepted as the ultimate failure point. The impact energy of the aggregates used was calculated from the RIHN test results. The hammer weighing 2.4 kg from a height of 63.5 cm was dropped onto the core samples (25.4 cm^3 volume core). The RIHN value was determined as the number of blows that resulted in 25% of the original core mass passing through the 0.5 mm sieve. Calculations were made using the same procedure as concrete impact energy calculation.

Table 3. Average test results of concrete mixtures.

Code	Aggregate Type	Rock Class	Concrete properties								
			CS _C MPa	STS _C MPa	LA _C %	SHH _C rebound	UPV _C km/sec	IE _C kJ	UW _C g/cm ³	WA _C %	Pg _C %
M ₁	Gabbro 1	Plutonic	41.7	3.43	14.2	27.7	4.84	0.31	2.49	3.85	9.4
M ₂	Andesite 1	Volcanic	42.0	2.78	14.0	26.0	4.83	0.24	2.27	4.20	9.5
M ₃	Gabbro 2	Plutonic	38.9	3.22	13.7	25.0	4.67	0.33	2.46	4.11	9.7
M ₄	Granite 1	Plutonic	42.1	3.32	13.3	29.0	4.51	0.22	2.30	4.57	10.1
M ₅	Basalt	Volcanic	45.0	3.49	13.5	28.8	4.63	0.28	2.30	4.20	9.7
M ₆	Granite 2	Plutonic	39.6	2.78	14.4	25.1	4.41	0.31	2.30	4.48	10.0
M ₇	Diorite	Plutonic	31.9	2.20	16.9	23.4	4.39	0.12	2.24	3.87	8.7
M ₈	Limestone 1	Sedimentary	33.4	2.59	18.3	24.8	4.70	0.13	2.32	3.75	8.7
M ₉	Limestone 2	Sedimentary	34.9	2.55	18.8	23.9	4.65	0.16	2.35	4.38	10.0
M ₁₀	Granite 3	Plutonic	41.1	3.06	16.4	24.8	4.60	0.18	2.31	3.93	8.9
M ₁₁	Andesite 2	Volcanic	37.6	2.59	19.9	25.7	4.26	0.12	2.14	5.16	10.9
M ₁₂	Claystone	Sedimentary	29.8	2.00	17.3	21.9	3.88	0.14	2.02	9.06	14.7
M ₁₃	Breccia	Sedimentary	43.0	3.17	17.2	28.4	4.67	0.18	2.35	4.35	10.0
M ₁₄	Travertine	Sedimentary	42.6	3.12	17.8	27.4	4.67	0.18	2.33	4.78	10.7
M ₁₅	Dacite	Volcanic	29.9	1.79	16.9	22.8	3.46	0.14	2.03	8.90	16.7
M ₁₆	Serpentinite	Metamorphic	33.8	2.36	18.4	23.4	4.12	0.10	2.33	4.89	11.0
M ₁₇	Onyx	Sedimentary	29.6	1.97	23.8	21.4	4.55	0.06	2.34	4.11	9.5
M ₁₈	Tuff	Pyroclastic	24.8	1.66	21.2	20.3	3.30	0.10	1.88	9.64	17.0
M ₁₉	Gypsum	Sedimentary	16.5	1.40	24.1	20.0	3.70	0.05	1.97	5.69	11.2
M ₂₀	Ignimbrite	Pyroclastic	12.6	1.37	20.2	21.0	2.97	0.04	1.84	12.85	22.6

STS_C is a measure of the resistance of concrete to longitudinal stress. The STS_C test was carried out using the STS test apparatus under TS EN 12390-6, 2010. STS were measured at 28 days, by using cubic specimens with a 10 cm side (Figure 5b). BTS_R tests were conducted on core samples under the ISRM, 2007. The diameter of the cores is 42 mm and the thickness is 27 mm. The constant loading rate applied to the samples was chosen as 200 N/s and the tensile load on the concretes was applied continuously such that failure will occur within 5 minutes of loading. The average of the test results, which was repeated seven times for all rock types, was given in Table 2.



Figure 5. Concrete/aggregate tests a) RIHN b) IE test apparatus c) IE specimens after ultimate failure d) BTS_R e) STSc f) STSc specimens after ultimate failure g) aggregate specimen after 500 revolution h) LA test machine i) and concrete specimen after 500 revolution j) CS_C and physical test samples k) SHH_C and l) UPV_C.

LA_R test was performed according to the test procedures described in ASTM C 131-01, 2006. In the test, 5000 grams of class C aggregate and eight steel spheres (approximately 3330 grams) were rotated together for 500 cycles. The crushed aggregate particles were sieved through a 1.7 mm sieve and the sieve material was calculated as a percentage of the original mass. For the LA test of concretes, a total of twelve samples were obtained by dividing three disc samples with a diameter of 100 mm and a thickness of 64 mm into four with a stone cutter. Concrete samples, such as aggregate samples, were rotated 500 cycles and the crushed samples were sieved through a 1.7 mm sieve. In the LA test of the concrete samples, no steel spheres were used, the samples were abraded by hitting the walls of the drum and each other (Figure 5c).

For CS_R tests, core samples with their ends cut parallel to each other and their surfaces precisely smoothed were used. Cylindrical concrete samples (100 mm diameter and 200 mm length) were cast for twenty different mix types and CS_C tests were carried out on these samples. The CS_C was measured at 28 days of curing time and five cylindrical specimens were used in the CS_C test for each concrete type (Figure 5d). The compression machine ELE-3000 kN (TS EN 12390-3, 2012) was used for the determination of the rock and concrete samples. The stress ratio was applied uniformly between 1.0-1.2 MPa/s until the rock or concrete was completely deformed. The mean compressive strength values given in Tables 2 and 3 were calculated by taking the average of five experiments.

4. Mineralogical and chemical assessment

Although this study mainly focuses on the estimation of the mechanical properties of concrete, the effects of the mineralogical and chemical properties of aggregates on concrete strength will be evaluated under this title in general terms. To determine the geological origins and types of the rocks, petrographic analysis was performed according to the TS EN 12407, 2013 standard. A polarized optical microscope (with a 100-2000 magnification range) was used to examine the prepared thin sections. Concretes with different compressive strengths can be obtained with the same type of cement and coarse aggregate properties from different geological origins (mineralogical composition, micro-roughness, compressive strength, structure, etc.) (Yılmaz & Tuğrul, 2012; Petrounias et al., 2018a). The above-listed physical, textural, and mineralogical properties of aggregates, which make up approximately 60-80% of the concrete volume, directly affect the compressive strength of concrete (Xing et al., 2015). Similarly, the fracture energy in concrete depends on the properties of the aggregate such as grain shape, texture, and mineralogy (Wu et al., 2001).

Figure 6 shows XRD graphs and Figure 7 shows thin-section images of three rocks formed by acidic magma. As can be seen from Table 1, the chemical composition of these three rocks is very similar in that they consist of magma of the same property. These rocks have a SiO₂ content of approximately 70% and an Al₂O₃ content of 15%. Despite the similarity in their chemical contents, the petrographic and physical properties of these rocks are quite different. The 28-day CS of the concretes produced with Granite, Andesite, and Tuff aggregates having a CS of 138, 96, and 19 MPa respectively are 42.1, 37.6, and 24.8 MPa. Granite, which is a depth rock, is formed by the interlock of large and resistant minerals such as quartz, biotite, and plagioclase. There are almost no pores and matrix material between the minerals. Andesite is the surface rock. It is observed that the coarse and fine crystals of quartz and plagioclase are dispersed in the matrix material. Tuff is an extrusive rock. Figure 7 shows the structure of the tuff, consisting of rock particles, altered minerals, numerous pores, and matrix material.

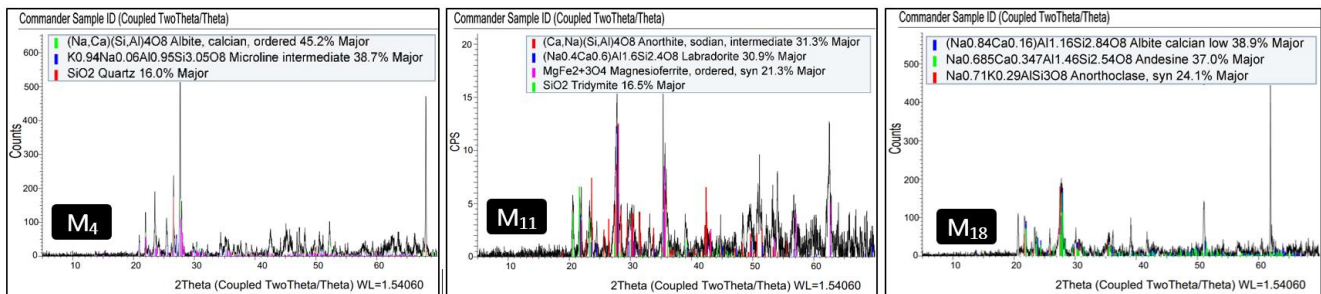


Figure 6. XRD graphs of some igneous aggregates (Granite-M₄, Andesite-M₁₁, and Tuff-M₁₈).

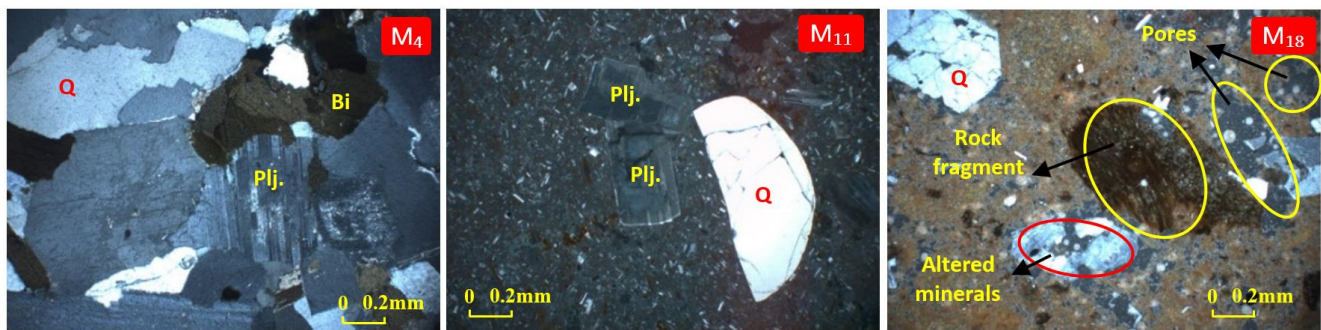


Figure 7. Thin section images of Granite (M₄), Andesite (M₁₁), and Tuff (M₁₈) rocks.

Aggregates have similar chemical and mineralogical properties but may have very different mechanical properties. These differences are mainly due to the heterogeneous structure of the aggregates. It is a reality that some aggregates react with cement paste due to their chemical structure to form a bond and contribute positively to concrete strength. However, this contribution is very limited and the main determinants of the strength are the coarse aggregate strength and the mechanical bond between the aggregate and cement paste. For a good bond; besides rough surface texture, mineralogically heterogeneous and porous grains are required. Figure 8 shows the XRD graphs of the three carbonate rocks. These rocks, which have very similar chemical properties with a CaO content of over 90%, are sedimentary in terms of geological origin. The 28-day CS of the concretes produced with Limestone, Travertine, and Onyx aggregate had a CS of 108, 77, and 22 MPa respectively 33.4, 42.6, and 29.6 MPa. The prominent parameter in this comparison is porosity and surface roughness rather than grain strength.

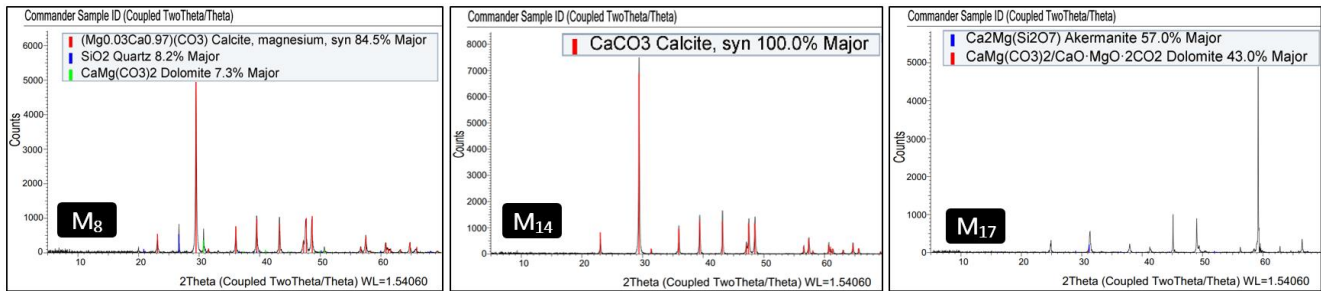


Figure 8. XRD graphs of some carbonated aggregates (Limestone-M₈, Travertine-M₁₄, and Onyx-M₁₇).

It is known from previous studies (French & Mokhtarzadeh, 1993; Özturan & Çeçen, 1997; Quiroga & Fowler, 2003; Al-Oraimi, Taha & Hassan, 2006; Rocco & Elices, 2008; Kamali-Bernard, Keinde & Bernard, 2014; Liu & Presuel-Moreno, 2014; Beushausen & Dittmer, 2015; Zunino, Castro & Lopez, 2015) that the coarse aggregate type can significantly affect the performance and properties of concrete. This effect is predominantly dependent on the microstructure and level of ITZ between coarse aggregate and mortar (Monteiro & Mehta, 1986; Hussin & Poole, 2011; Kamali-Bernard, Keinde & Bernard, 2014). This bond can be affected by the physical properties of aggregates such as roughness, shape, angularity and chemical properties such as reactivity (Miller et al., 2011). Alteration degrees, mineralogical composition of aggregates strongly affect their in-service performance and mechanical behavior (Al-Oraimi, Taha & Hassan, 2006; Rigopoulos et al., 2010; Yılmaz, Goktan & Kibici, 2011; Yılmaz & Tuğrul, 2012; Petrounias et al., 2016; Petrounias et al., 2018b). Flat or fibrous crystals, increased secondary mineral percentages, smooth layers and cleavage of aggregates adversely affect the physical and mechanical properties of aggregates and the concrete produced from them (Petrounias et al., 2018b).

As can be seen from Figure 2, different rocks can have very different grain shapes when subjected to crushing. When a laminated rock breaks, a large number of defective grains (flat-long) is produced, whereas more cubic-shaped particles are formed when the rock which a more homogeneous structure breaks. The statistical analyses carried out with the results of the laboratory tests showed that the mechanical and physical properties of the aggregates are directly related to the properties of the produced concrete. Parameters such as grain strength, porosity, grain shape, and density contribution to the concrete strength separately, but the ideal aggregate should have a large part of these properties. CS_R of the M₈-Micritic Limestone (108 MPa) is approximately 2 times that of the M₁₅-Dacite (65 MPa). The compressive strength of the concretes produced with these aggregates is equal. The main reason for this is the conchoidal breakage of the M₈-aggregate and the smoothness of these fractured surfaces. Since there is not enough adherence between the cement paste and the aggregate surface, failure occurs at this interface. In this case, the grain strength alone is not enough. Crushed stone, which can develop a greater mechanical bond with cement paste due to its angular structure and rough surface, provides higher strength than gravel (Al-Oraimi, Taha & Hassan, 2006). The roughness of the aggregate surface significantly increases the fracture energy of the interface, the nature of which depends on the microstructure properties of the aggregate (Zhang & Gjørsv, 1990). The type of rock surface significantly affects the interfacial properties of composite materials (Alexander, 1993). In the case of the porous surface, hydration products penetrate the pores, leading to an increase in mechanical locking. M₁₂-Claystone and M₁₃-Breccia have the same compressive strength. However, the concrete produced by M₁₃ showed about 50% more strength than the concrete produced by M₁₂. The main problem here arises from the grain shape of the Claystone. The crushed stone, which is made of layered claystone, contains a large amount of flat and long grains. The grain shape of the M₁₃-Breccia aggregates is more cubic. The failure of the concrete produced by Claystone is due to the weak shear strength of the coarse aggregates.

The physicomaterial properties of an aggregate depend on the degree of alteration and deformation of the rock from which it is produced, and its petrographic properties (mineralogical composition, texture, size, shape, arrangement, and degree of interlocking) (Tuğrul & Zarif, 1999; Miskovsky et al., 2004). The properties of an ITZ are affected by the shape, surface texture, and composition of coarse aggregates, which play an important role in the mechanical behavior of concrete (Zhang & Gjørsv, 1990; Alexander, 1993; Hong, Gu & Lin, 2014; Qudoos et al., 2018). Another comparison can be made for M₁ (Gabbro 1) and M₅ (Basalt) rocks. M₁ has a CS_R of 233 MPa while M₅ has a CS_R of 136 MPa. Despite this 70% strength difference, the concrete produced with M₅ gave higher CS_C than the concrete produced with M₁. Gabbro is a rock formed by

the combination of coarse and resistant mineral grains, but it is quite nonporous. M₅-Basalt is a volcanic rock with a reasonable amount of pores, in which strong mineral grains come together with a strong cement material (Figure 9). Cement pulp enters the recesses and pores of the crushed stone aggregate produced from basalt and the aggregate protrusions sink into the cement paste. In general, a wedge-shaped coupling occurs. Although M₁-aggregates consist of more resistant particles, the pored structure of the M₅ aggregate leads to a higher concrete strength.

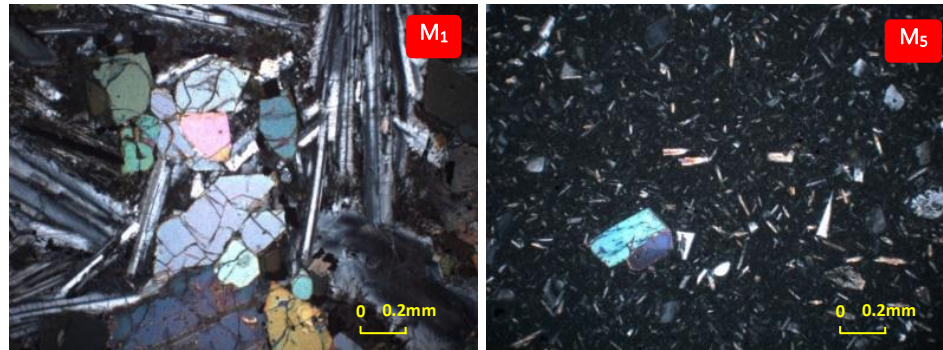


Figure 9. Thin section images of M₁ (Gabbro) and M₅ (Basalt) rocks.

5. Statistical analysis and results

The enter technique in (SPSS v.17.0) statistical software package was used to develop the most successful regression models that can predict concrete properties from aggregate/rock properties. In this context, two different methods, simple regression analysis, and non-linear multiple regression analysis, were preferred for the analysis of data obtained from experimental studies. First of all, simple regression analysis was performed to investigate the weight of each test that will be the input parameter in the models intended to be obtained using nonlinear functions. To test the relationships between concrete properties and similar rock properties, first, the best nonlinear curve estimations were determined, trying linear [Y = a + bx], logarithmic [Y = a + bln(x)], inverse [Y = a + (b/x)], quadratic [Y = a + bx + cx²], cubic [Y = a + bx + cx² + dx³], compound [Y = ab^x], power [Y = ax^b], S-curve [Y = e^{(a+(b/x))}], growth [Y = e^(a+bx)], exponential [Y = ae^(bx)] and logistic [Y = 1 / (1/u + ab^x)] fittings for dataset (Table 4 and Figures 10-18).

Table 4. The best-fit equations validated by R², F, and t-tests (|t|_{tabulated} = 2.26 and F_{tabulated} = 4.41)

Equations number	Dependent variables	Indep. variables	Best fit model	F ratio	p value	t constant	p value	t indep.(a)	p value	t indep.(b)	p value	t indep.(c)	p value	R ²
Equation (1)	CSc	CSR	S-Curve	92.4	0.00	98.5	0.00	9.6	0.00	*	*	*	*	0.837
Equation (2)	STSc	BTSR	Power	55.6	0.00	11.4	0.00	7.5	0.00	*	*	*	*	0.755
Equation (3)	LAc	LAR	Power	78.5	0.00	6.6	0.00	8.9	0.00	*	*	*	*	0.814
Equation (4)	SHHc	SHHR	Exponential	32.6	0.00	15.3	0.00	5.7	0.00	*	*	*	*	0.644
Equation (5)	UPVc	UPVR	Power	103.4	0.00	25.8	0.00	10.2	0.00	*	*	*	*	0.852
Equation (6)	IEc	IER-RIHN	Power	91.3	0.00	12.1	0.00	9.6	0.00	*	*	*	*	0.835
Equation (7)	UWc	UWR	Exponential	234.5	0.00	28.6	0.00	15.3	0.00	*	*	*	*	0.929
Equation (8)	WAc	WAR	Cubic	48.6	0.00	13.0	0.00	5.6	0.00	5.6	0.00	6.3	0.00	0.901
Equation (9)	Pgc	PGR	Cubic	40.7	0.00	18.6	0.00	3.3	0.01	3.2	0.01	4.0	0.00	0.884

$$CSc = e^{(3.711 - \frac{8.722}{CSR})} \quad (R^2=0.837) \quad (1)$$

$$BTS_C = 1.34 STS_R^{0.323} \quad (R^2=0.755) \quad (2)$$

$$LAc = 4.543 LA_R^{0.391} \quad (R^2=0.814) \quad (3)$$

$$SHH_C = 16.981 e^{0.008 SHH_R} \quad (R^2=0.644) \quad (4)$$

$$UPV_C = 2.929 UPV_R^{0.268} \quad (R^2=0.852) \quad (5)$$

$$IE_C = 0.262 IE_{R-RIHN}^{0.696} \quad (R^2=0.835) \quad (6)$$

$$UW_C = 1.308 e^{0.218 UW_R} \quad (R^2=0.929) \quad (7)$$

$$WA_C = 0.007WA_R^3 - 0.203WA_R^2 + 1.714WA_R + 3.626 \quad (R^2=0.901) \quad (8)$$

$$Pg_C = 0.002Pg_R^3 - 0.09Pg_R^2 + 1.181Pg_R + 8.76 \quad (R^2=0.884) \quad (9)$$

Some test values of aggregate rock were significantly correlated with similar values of concretes. The correlation coefficients obtained from the simple equations established to predict the concrete properties varied between 0.64 and 0.93. While the weakest correlation between the six tests was obtained from the SHH test (Equation 4), the highest correlation coefficient (Equation 7) was obtained by UW values.

The histogram graphs (a), simple regression lines (b), and scatter plots (c) for concretes were shown in Figures 10-18. The histogram graphics in Figures 10a-18a allow us to compare the same properties of aggregates and hardened concrete produced from those aggregates. Figures 10b-18b present the curves of the best-fit models with minimum/maximum confidence intervals and minimum/maximum prediction intervals. Correlation plots clearly represent the nonlinear relationship between each concrete property and aggregate property. Figure 10c-18c allows a comparison of the results of concrete tests from laboratory studies with the results obtained from the estimates. The fit of the line representing the relationship between measurement and prediction to the 1:1 line represents the predictive power of this correlation.

95% confidence interval values were calculated to check the validity of the derived equations. The validity and significance of the equations obtained by the statistical studies are shown by F and t-tests (Table 4). The significance level of the correlation coefficients was determined by t-test. It was observed that all t-values of the equations were greater than the table t-value (2.26). Similarly, all of the significance values (*p-value*) are less than 0.05. It was observed that the F-values obtained by the regression analysis of variance were considerably larger than the table F value (4.41). These equations, which are estimated using a single independent variable, are more practical than equations containing more than one independent variable and can be used especially for prediction purposes.

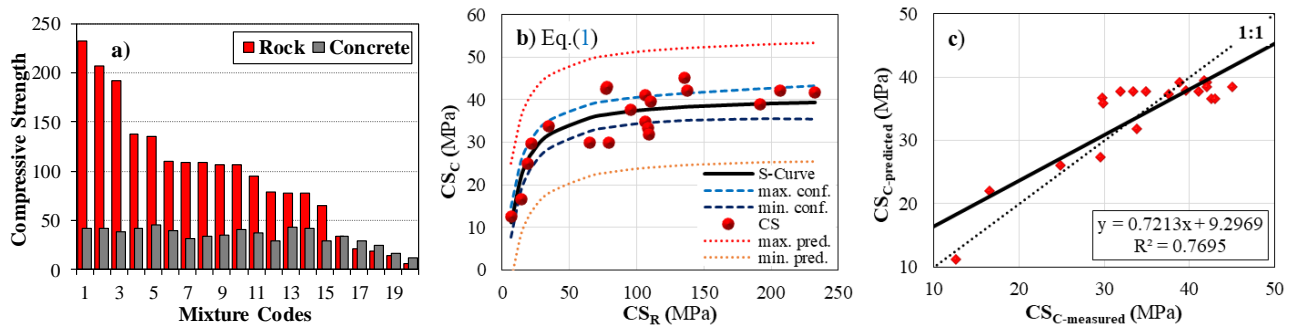


Figure 10. a) Histogram graph of CS_R and CS_C , b) correlation between CS_R and CS_C for Equation 1, and c) comparison of CS_C -measured and CS_C -predicted for Equation 1.

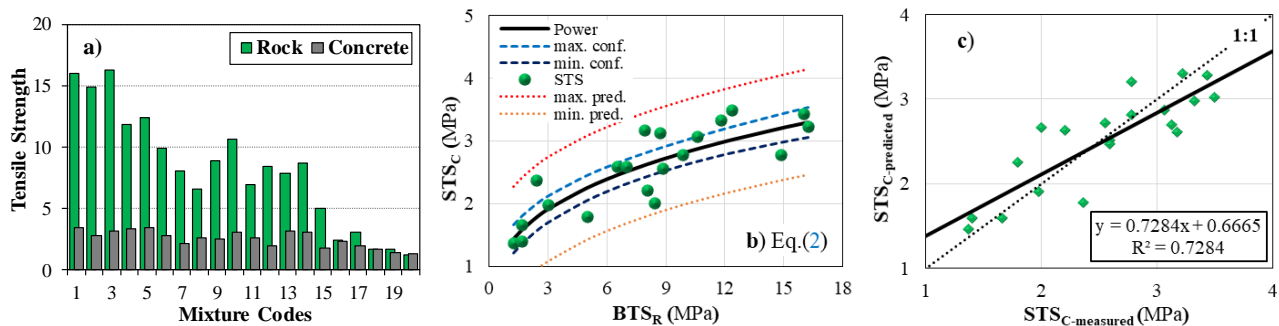


Figure 11. a) Histogram graph of BTS_R and STS_C , b) correlation between BTS_R and STS_C for Equation 2, and c) comparison of STS_C -measured and STS_C -predicted for Equation 2.

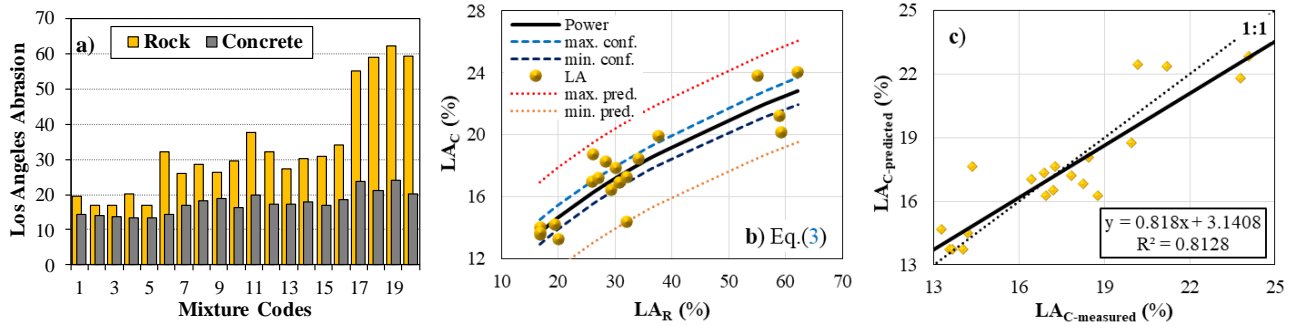


Figure 12. a) Histogram graph of LAR and LAC , b) correlation between LAR and LAC for Equation 3, and c) comparison of LAC -measured and LAC -predicted for Equation 3.

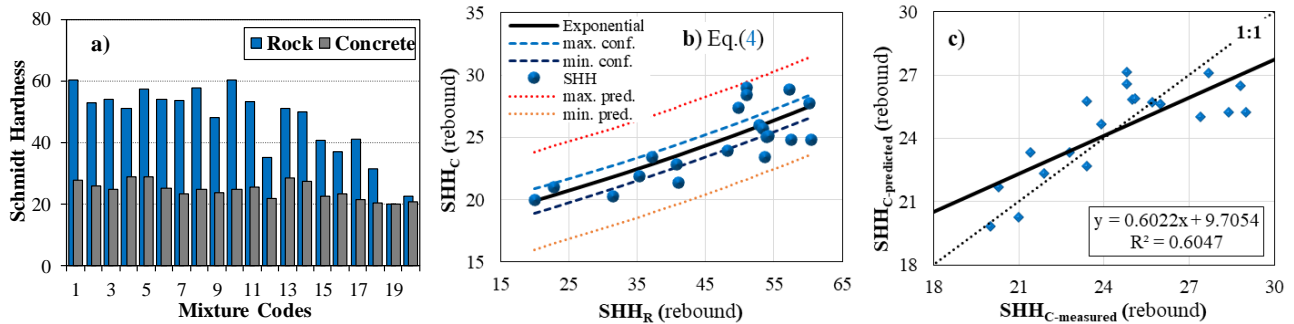


Figure 13. a) Histogram graph of $SHHR$ and $SHHC$, b) correlation between $SHHR$ and $SHHC$ for Equation 4, and c) comparison of $SHHC$ -measured and $SHHC$ -predicted for Equation 4.

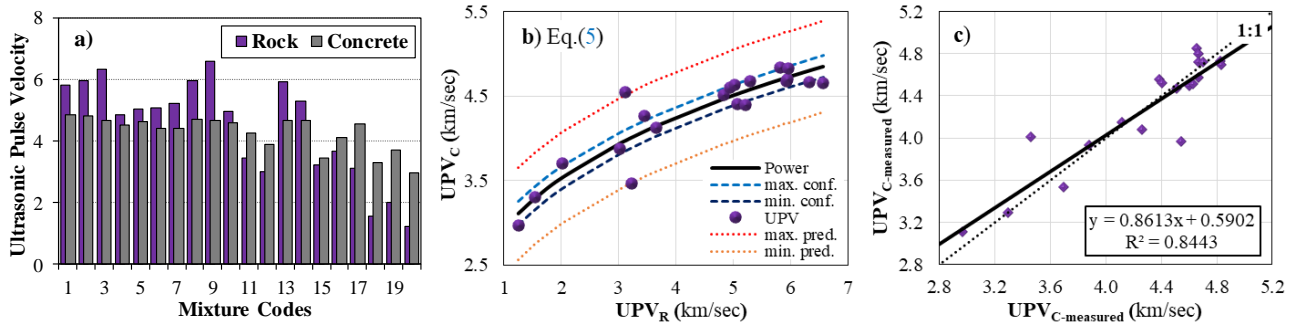


Figure 14. a) Histogram graph of $UPVR$ and $UPVC$, b) correlation between $UPVR$ and $UPVC$ for Equation 5, and c) comparison of $UPVC$ -measured and $UPVC$ -predicted for Equation 5.

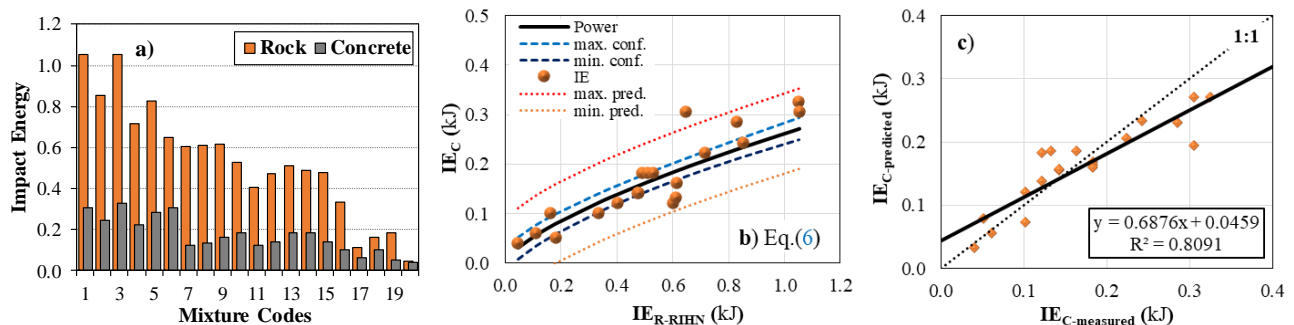


Figure 15. a) Histogram graph of IER -RH and IEC , b) correlation between IER -RH and IEC for Equation 6, and c) comparison of IEC -measured and IEC -predicted for Equation 6.

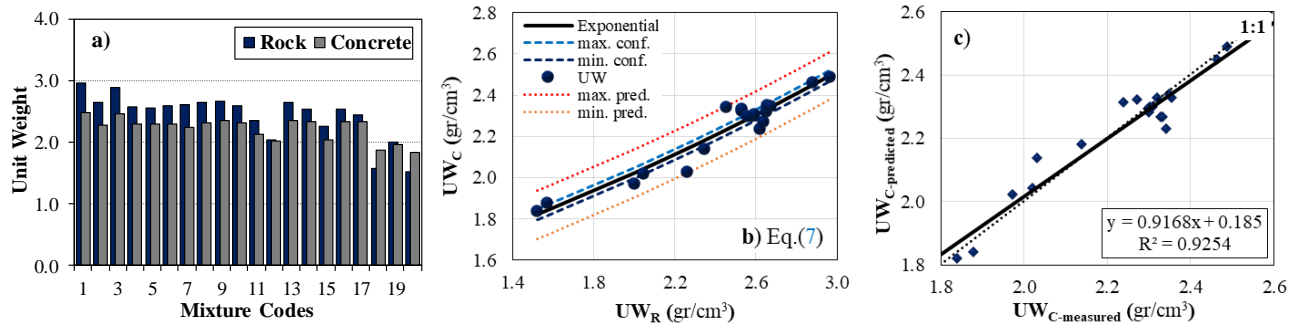


Figure 16. a) Histogram graph of UW_R and UW_C , b) correlation between UW_R and UW_C for Equation 7, and c) comparison of $UW_{C\text{-measured}}$ and $UW_{C\text{-predicted}}$ for Equation 7.

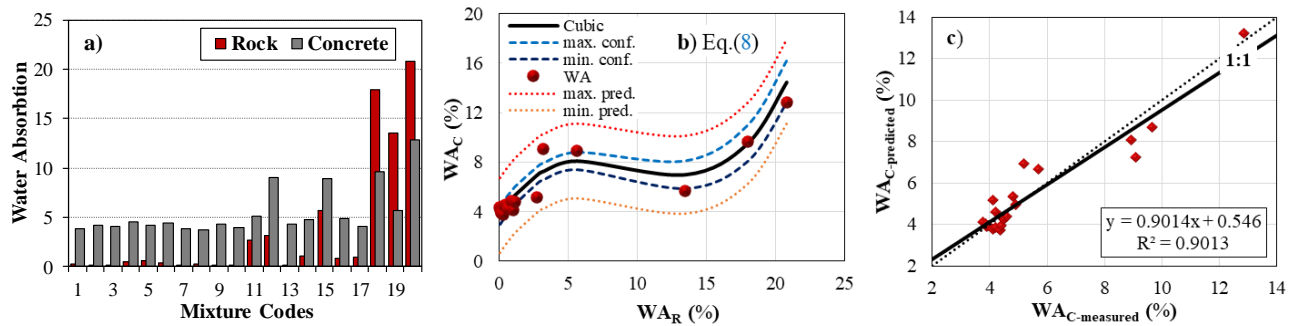


Figure 17. a) Histogram graph of WA_R and WA_C , b) correlation between WA_R and WA_C for Equation 8, and c) comparison of $WA_{C\text{-measured}}$ and $WA_{C\text{-predicted}}$ for Equation 8.

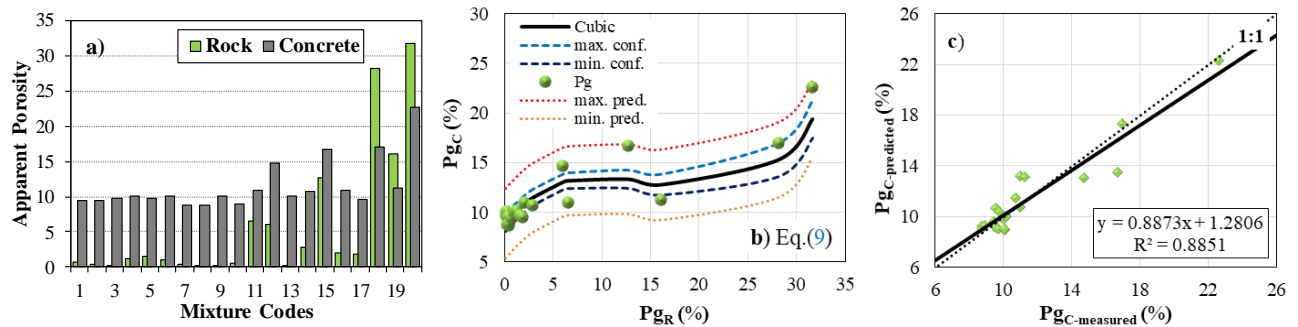


Figure 18. a) Histogram graph of Pg_R and Pg_C , b) correlation between Pg_R and Pg_C for Equation 9, and c) comparison of $Pg_{C\text{-measured}}$ and $Pg_{C\text{-predicted}}$ for Equation 9.

In the second stage of regression analyses, a series of nonlinear multiple regression analyses were performed to predict main concrete properties (CS_C , STS_C , LA_C , and IE_C). The hardness, strength, and various physical properties of the aggregate as well as the binder material have a significant effect on the concrete strength. While creating multiple regression models, it was assumed that the mechanical properties of concrete are a complex problem that is affected by many aggregate properties. Nonlinear regression is a method used to find a nonlinear model of the relationship between a feature determined as the dependent variable and a set of independent variables. Unlike traditional regression, which is limited to the estimation of only linear models, a model with arbitrary relationships between dependent and independent variables can be obtained with the help of nonlinear regression. Multiple nonlinear regression is one of the methods in which Y-dependent values are estimated based on given independent values (Tiryaki, 2008). In this study, the twin logarithmic method was used in multivariate nonlinear regression analysis for the estimation (Choi, 1978). The parameters used in simple regressions were analyzed in various combinations using the equation described below, and the process was performed using an iterative estimation algorithm. The equation is as follows:

$$Y=aX_1^{b1} X_2^{b2} \dots\dots\dots X_n^{bn}$$

Where Y is the dependent variable, a is the intercept, X₁, X₂, and the X_n are independent variables and b₁, b₂, and b_n are the regression equation constants. The generated nonlinear multiple regression models (Model 1, Model 2, and Model 3) are shown schematically in Figure 19. Accordingly, for all three models, one of the CS_C, STS_C, LA_C, and IE_C was defined as the dependent variable, and estimation was made with the help of four independent variables. Again for all three models, aggregate tests (CS_R, BTS_R, LA_R, and IER-RIHN) with the same principles as these concrete properties were used as the first independent variable. The two, third, and fourth independent variables for Model 1 consist of concrete properties. SHH_C and UPV_C tests were used as the second and third independent variables, respectively. As the fourth independent variable, one of the physical properties of concrete (UW_C, WA_C, and Pg_C) was used in the model. Model (1), Model (2), and Model (3) are built on the same principles. Model (2), it is aimed to predict basic concrete properties using only aggregate/rock properties. The second, third, and fourth independent variables in Model (3) are based on choosing one of the aggregate or concrete properties that provide the strongest coefficient of determination.

Nonlinear Multiple Regression MODEL 1													
OUTPUT Concrete Properties				INPUT (1) Similar Rock Properties				INPUT (2) Concrete Hardness		INPUT (3) Concrete	INPUT (4) Concrete Physical		
CS _C	STS _C	LA _C	IE _C	CS _R	STS _R	LA _R	IER-RIHN	SHH _C		UPV _C	UW _C Pg _C		
Nonlinear Multiple Regression MODEL 2													
OUTPUT Concrete Properties				INPUT (1) Similar Rock Properties				INPUT (2) Rock Hardness		INPUT (3) Rock	INPUT (4) Rock Physical		
CS _C	STS _C	LA _C	IE _C	CS _R	STS _R	LA _R	IER-RIHN	SHH _R		UPV _R	UW _R Pg _R		
Nonlinear Multiple Regression MODEL 3													
OUTPUT Concrete Properties				INPUT (1) Similar Rock Properties				INPUT (2) Concrete/Rock Hardness		INPUT (3) Concrete/Rock		INPUT (4) Concrete/Rock Physical	
CS _C	STS _C	LA _C	IE _C	CS _R	STS _R	LA _R	IER-RIHN	SHH _C	SHH _R	UPV _C	UPV _R	UW _R UW _C Pg _R Pg _C	

Figure 19. Schematic representation of nonlinear multiple regression models

$CS_C=0.335 \times CS_R^{0.074} \times SHH_C^{1.05} \times UPV_C^{0.57} \times UW_C^{0.143}$	(Model-1)	($R^2=0.875$)	(10)
$CS_C=2.798 \times CS_R^{0.046} \times SHH_R^{0.559} \times UPV_R^{0.104} \times UW_R^{0.022}$	(Model-2)	($R^2=0.808$)	(11)
$CS_C=0.329 \times CS_R^{0.074} \times SHH_C^{1.051} \times UPV_C^{0.667} \times UW_R^{0.016}$	(Model-3)	($R^2=0.875$)	(12)
$CS_C=0.183 \times CS_R^{0.072} \times SHH_C^{0.99} \times UPV_C^{0.953} \times Pg_C^{0.152}$	(Model-1)	($R^2=0.877$)	(13)
$CS_C=2.146 \times CS_R^{-0.003} \times SHH_R^{0.553} \times UPV_R^{0.449} \times Pg_R^{0.07}$	(Model-2)	($R^2=0.841$)	(14)
$CS_C=0.298 \times CS_R^{0.079} \times SHH_C^{0.988} \times UPV_C^{0.846} \times Pg_R^{0.016}$	(Model-3)	($R^2=0.878$)	(15)

The results of the constructed different equations were plotted on a scatterplot showing the target (measured) versus the model (predicted). Plotting the data points for the predicted versus measured output against a (1:1) line is the best way of finding out the prediction capacity of the models. The point that lies on the (1:1) line shows the exact prediction of the output by the model and the closer a point to the (1:1) line, the better the prediction. Figures 20-23 are plotted for concrete's CS, STS, LA, and IE properties, respectively. The plotted points were lying close to the (1:1) line implying a successful prediction of all models.

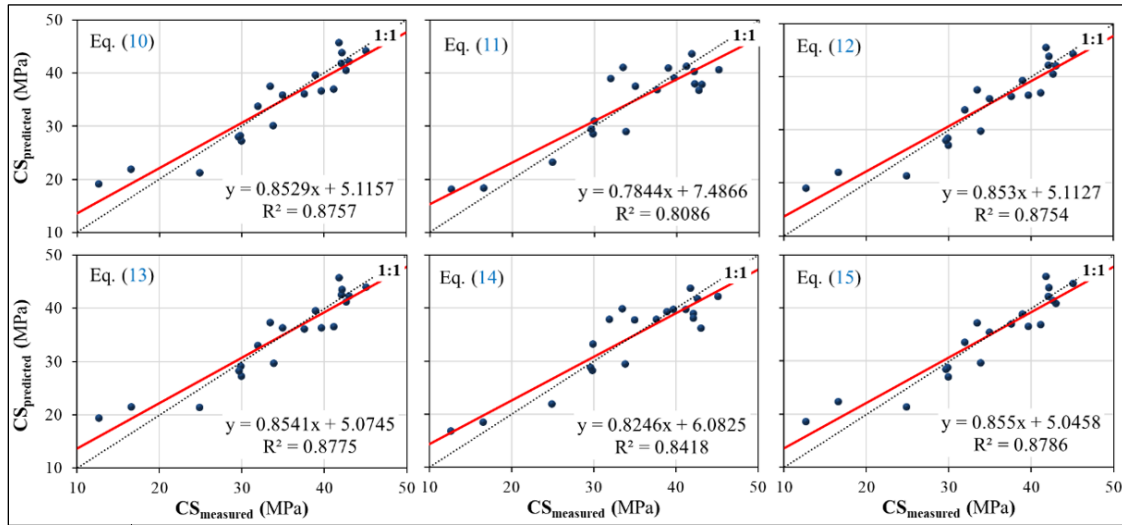


Figure 20. Comparison of predicted and measured values for Equations (10-15) (CS_c).

$STS_C = 0.013 \times BTS_R^{0.088} \times SHH_C^{1.309} \times UPV_C^{-0.073} \times UW_C^{1.211}$ (Model-1)	$(R^2 = 0.958)$	(16)
$STS_C = 0.317 \times BTS_R^{0.154} \times SHH_R^{0.379} \times UPV_R^{-0.027} \times UW_R^{0.412}$ (Model-2)	$(R^2 = 0.806)$	(17)
$STS_C = 0.011 \times BTS_R^{0.110} \times SHH_C^{1.303} \times UPV_C^{-0.105} \times UW_C^{1.436}$ (Model-3)	$(R^2 = 0.961)$	(18)
$STS_C = 0.015 \times BTS_R^{0.086} \times SHH_C^{1.343} \times UPV_C^{0.541} \times P_{g_C}^{-0.044}$ (Model-1)	$(R^2 = 0.938)$	(19)
$STS_C = 0.285 \times BTS_R^{0.129} \times SHH_R^{0.408} \times UPV_R^{0.247} \times P_{g_R}^{0.031}$ (Model-2)	$(R^2 = 0.806)$	(20)
$STS_C = 0.012 \times BTS_R^{0.084} \times SHH_C^{1.334} \times UPV_C^{0.614} \times P_{g_R}^{-0.001}$ (Model-3)	$(R^2 = 0.938)$	(21)

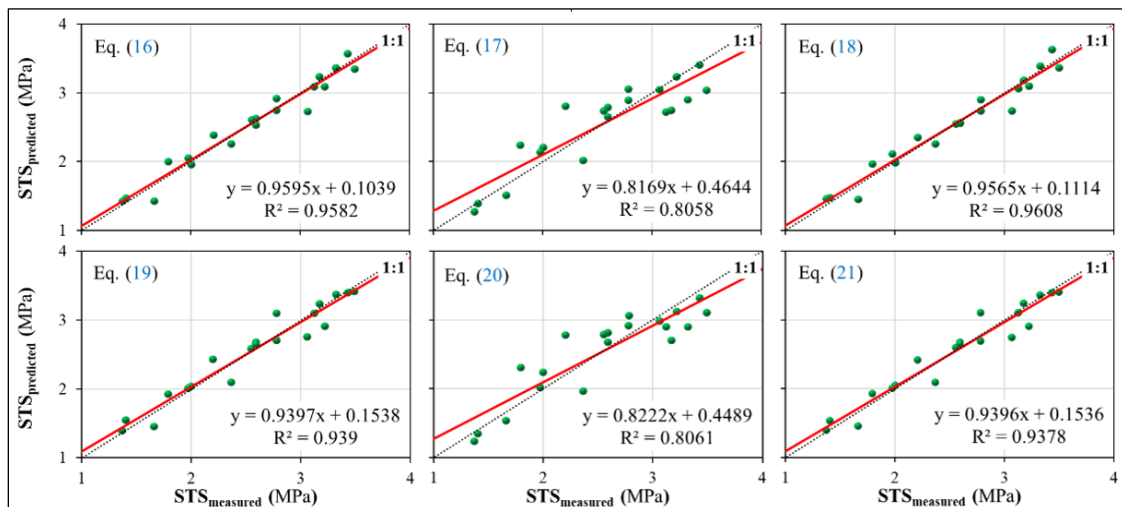


Figure 21. Comparison of predicted and measured values for Equations (16-21) (STS_c).

$LA_C = 6.583 \times LA_R^{0.417} \times SHH_C^{0.362} \times UPV_C^{-0.674} \times UW_C^{-0.344}$ (Model-1)	$(R^2 = 0.892)$	(22)
$LA_C = 3.152 \times LA_R^{0.529} \times SHH_R^{0.113} \times UPV_R^{0.169} \times UW_R^{0.103}$ (Model-2)	$(R^2 = 0.881)$	(23)
$LA_C = 6.696 \times LA_R^{0.424} \times SHH_C^{0.367} \times UPV_C^{0.445} \times UW_R^{0.034}$ (Model-3)	$(R^2 = 0.889)$	(24)
$LA_C = 5.586 \times LA_R^{0.422} \times SHH_C^{0.395} \times UPV_C^{0.581} \times P_{g_C}^{0.046}$ (Model-1)	$(R^2 = 0.889)$	(25)
$LA_C = 3.290 \times LA_R^{0.536} \times SHH_R^{0.117} \times UPV_R^{0.200} \times P_{g_R}^{-0.004}$ (Model-2)	$(R^2 = 0.880)$	(26)
$LA_C = 6.746 \times LA_R^{0.418} \times SHH_C^{0.375} \times UPV_C^{0.492} \times P_{g_R}^{0.001}$ (Model-3)	$(R^2 = 0.889)$	(27)

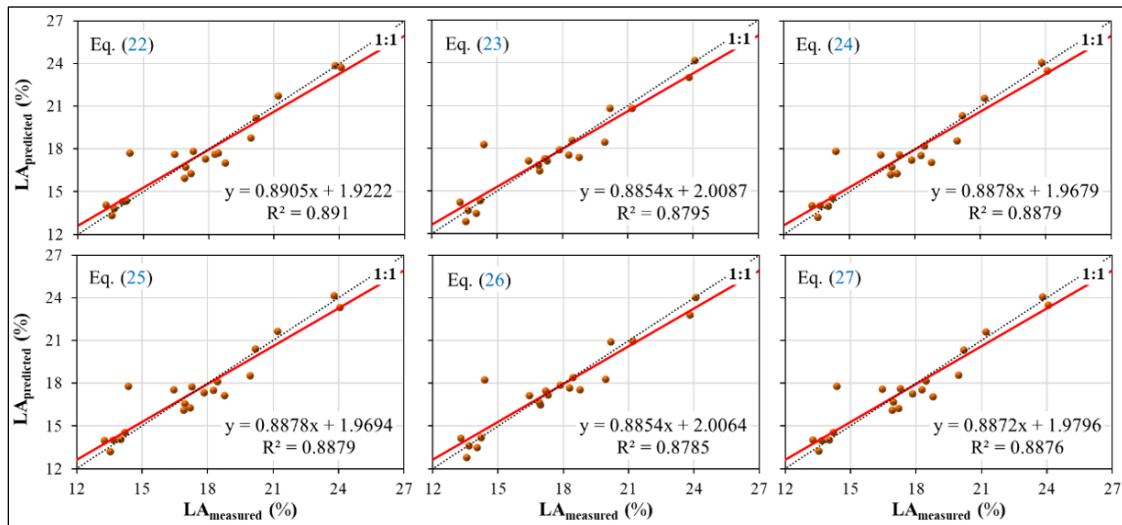


Figure 22. Comparison of predicted and measured values for Equations (22-27) (LAc).

$IE_C = 0.028 \times IE_{R-RIHN}^{0.807} \times SHH_C^{0.930} \times UPV_C^{-1.317} \times UW_C^{1.565}$	(Model-1)	(R ² =0.844)	(28)
$IE_C = 0.158 \times IE_{R-RIHN}^{0.982} \times SHH_R^{0.335} \times UPV_R^{-0.256} \times UW_R^{-0.246}$	(Model-2)	(R ² =0.828)	(29)
$IE_C = 0.029 \times IE_{R-RIHN}^{0.873} \times SHH_C^{0.562} \times UPV_R^{-0.442} \times UW_C^{1.469}$	(Model-3)	(R ² =0.845)	(30)
$IE_C = 0.005 \times IE_{R-RIHN}^{0.864} \times SHH_C^{0.765} \times UPV_C^{0.301} \times P_{gC}^{0.463}$	(Model-1)	(R ² =0.840)	(31)
$IE_C = 0.117 \times IE_{R-RIHN}^{0.922} \times SHH_R^{0.242} \times UPV_R^{0.006} \times P_{gR}^{0.051}$	(Model-2)	(R ² =0.830)	(32)
$IE_C = 0.011 \times IE_{R-RIHN}^{0.894} \times SHH_C^{0.812} \times UPV_R^{-0.052} \times P_{gC}^{0.306}$	(Model-3)	(R ² =0.839)	(33)

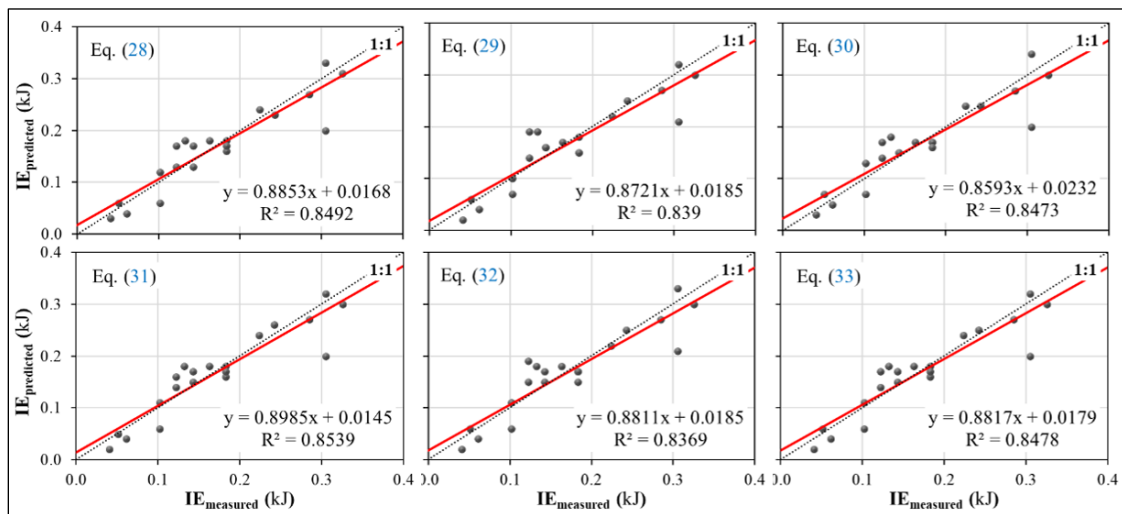


Figure 23. Comparison of predicted and measured values for Equations (28-33) (IE_C).

Anova analysis was applied for comparison of the generated multiple equations with each other. The comparison was made using the data of six equations produced under the same conditions for the estimation of each of the basic concrete properties. The variations of the measured and predicted values were also tested using one-way analysis of variance (Anova) and found to be perfect (CS_C; Levene statistic: 0.023 and significance: 1, STS_C; Levene statistic: 0.065 and significance: 1, LA_C; Levene statistic: 0.064 and significance: 1, IE_C; Levene statistic: 0.104 and significance: 1).

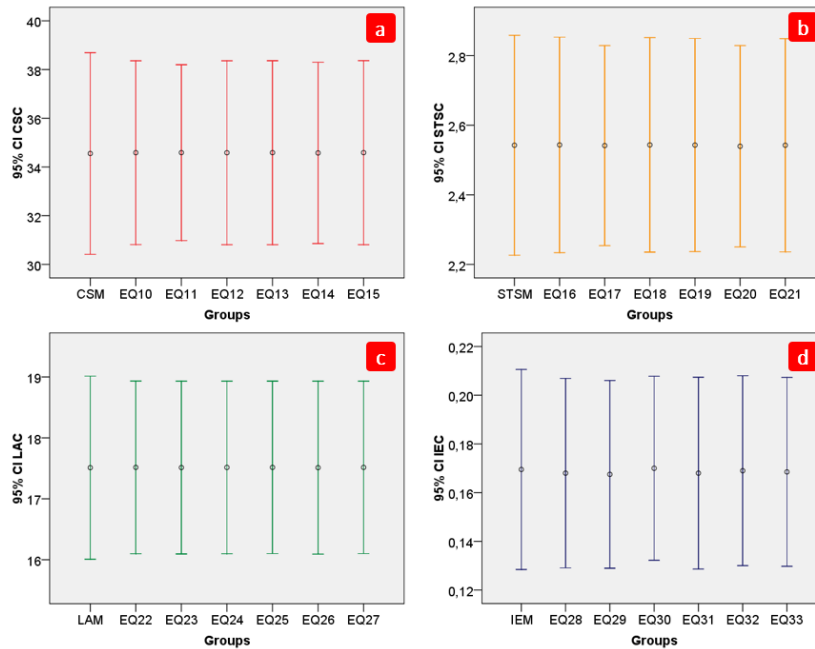


Figure 24. Comparison of the mean values of the nonlinear regression equations a) CS_C b) STS_C c) LA_C and d) IE_C.

Table 5. Multiple comparisons of the measured and predicted test values for NMRA.

Eqs. no	PI _{at}	(I)	(J)	Mean Difference (I-J)	Std. Error	Sig.	Dunnnett t (2-sided) ^a	
							99.762 % Confidence Interval	
							Lower Bound	Upper Bound
(Compressive Strength of Concrete) CS_C								
Equation (10)	2.236	CS _{predicted}	CS _{measured}	0.0330	2.5670	1.0000	-9.2392	9.3052
Equation (11)	1.932	CS _{predicted}	CS _{measured}	0.0355	2.5670	1.0000	-9.2367	9.3077
Equation (12)	2.235	CS _{predicted}	CS _{measured}	0.0325	2.5670	1.0000	-9.2397	9.3047
Equation (13)	2.245	CS _{predicted}	CS _{measured}	0.0340	2.5670	1.0000	-9.2382	9.3062
Equation (14)	2.081	CS _{predicted}	CS _{measured}	0.0225	2.5670	1.0000	-9.2497	9.2947
Equation (15) [*]	2.250	CS _{predicted}	CS _{measured}	0.0355	2.5670	1.0000	-9.2367	9.3077
(Splitting Tensile Strength of Concrete) STS_C								
Equation (16)	2.640	STS _{predicted}	STS _{measured}	0.0010	0.2051	1.0000	-0.7398	0.7418
Equation (17)	1.887	STS _{predicted}	STS _{measured}	-0.0010	0.2051	1.0000	-0.7418	0.7398
Equation (18) [*]	2.656	STS _{predicted}	STS _{measured}	0.0010	0.2051	1.0000	-0.7398	0.7418
Equation (19)	2.533	STS _{predicted}	STS _{measured}	0.0005	0.2051	1.0000	-0.7403	0.7413
Equation (20)	1.886	STS _{predicted}	STS _{measured}	-0.0030	0.2051	1.0000	-0.7438	0.7378
Equation (21)	2.526	STS _{predicted}	STS _{measured}	0.0000	0.2051	1.0000	-0.7408	0.7408
(Los Angeles Abrasion of Concrete) LA_C								
Equation (22) [*]	2.311	LA _{predicted}	LA _{measured}	0.0045	0.9660	1.0000	-3.4848	3.4938
Equation (23)	2.257	LA _{predicted}	LA _{measured}	0.0015	0.9660	1.0000	-3.4878	3.4908
Equation (24)	2.297	LA _{predicted}	LA _{measured}	0.0035	0.9660	1.0000	-3.4858	3.4928
Equation (25)	2.296	LA _{predicted}	LA _{measured}	0.0045	0.9660	1.0000	-3.4848	3.4938
Equation (26)	2.252	LA _{predicted}	LA _{measured}	0.0000	0.9660	1.0000	-3.4893	3.4893
Equation (27)	2.295	LA _{predicted}	LA _{measured}	0.0040	0.9660	1.0000	-3.4853	3.4933
(Impact Energy of Concrete) IE_C								
Equation (28)	1.103	IE _{predicted}	IE _{measured}	-0.0015	0.0264	1.0000	-0.0969	0.0939
Equation (29)	0.980	IE _{predicted}	IE _{measured}	-0.0020	0.0264	1.0000	-0.0974	0.0934
Equation (30)	1.115	IE _{predicted}	IE _{measured}	0.0005	0.0264	1.0000	-0.0949	0.0959
Equation (31) [*]	1.131	IE _{predicted}	IE _{measured}	-0.0015	0.0264	1.0000	-0.0969	0.0939
Equation (32)	0.908	IE _{predicted}	IE _{measured}	-0.0005	0.0264	1.0000	-0.0959	0.0949
Equation (33)	1.047	IE _{predicted}	IE _{measured}	-0.0010	0.0264	1.0000	-0.0964	0.0944

a. Dunnnett t-tests treat one group as a control, and compare all other groups against it.

According to the Anova test results, there was no difference between the mean values between the groups and the mean values within the groups (CS_C ; F statistic: 0.000 and significance: 1, STS_C ; F statistic: 0.000 and significance: 1, LA_C ; F statistic: 0.000 and significance: 1, IE_C ; F statistic: 0.002 and significance: 1). Dunnett two-sided T-test, one of the post-hoc tests, was used for comparison of nonlinear multiple equations. In this way, it was possible to compare each of the models derived for CS_C , STS_C , LA_C , and IE_C within itself. The test results revealing the relationships between the measured and predicted values are given in Table 5 and Figure 24. It is seen that each data pair has very close mean differences and equal standard error values. This shows that the mechanical properties of hardened concrete (CS_C , STS_C , LA_C , and IE_C) can be reliably predicted from any equation.

Dunnett's two-sided T-test showed that all data pairs had an equal level of standard error and significance level, and the mean differences were very close to each other. This shows that these equations can be used to reliably estimate the CS, STS, LA, and IE of concrete. It is quite difficult to choose the most accurate and powerful model among the many derived equations for the estimation of any dependent variable. In the literature, the accuracy of prediction models is examined separately using statistical performance indices such as WMAPE, VAF, RMSE, RSR, and R^2 . In order to establish a stronger and more accurate selection criterion, a performance index (PI_{at}) previously developed by the author and published by the author was used (Teymen & Mengüç, 2020). In the last step of the statistical analysis, the capacity performance of the derived equations for estimation was checked using this index.

Theoretically, the PI_{at} value of excellent prediction models is equal to 3 as expected. The PI_{at} values of all estimation equations are given in the second column of Table 5. According to this criterion, the equations with the highest predictive power for CS, STS, LA, and IE are Equation 15, Equation 18, Equation 22, and Equation 31, respectively. To determine which test method has the strongest prediction equations among these four main concrete properties, the average of the PI_{at} values of the six equations belonging to each concrete property was taken. Accordingly, while the equations with the highest predictive power were obtained for the STS_C (mean PI_{at} value: 2.35), LA_C (mean PI_{at} value: 2.28), and CS_C (mean PI_{at} value: 2.16) properties, respectively, the equations with the weakest predictive power were determined for the IE_C (mean PI_{at} value: 1.05) property.

6. Conclusions and comments

In this paper, the effect of the physical and mechanical properties of the aggregate rocks on some concrete properties was investigated. The following conclusions may be deduced from this study:

The simple relationships between the properties of hardened concrete and the similar properties of aggregates/rocks were examined in terms of nine different parameters. Strong and positive relationships were found in all of these examined parameters. The strongest and most general finding that can be drawn from simple regression analysis is that the improvement of aggregate quality affects increasing the strength of concrete.

Granite, Andesite, and Tuff are acidic magma-product rocks. For this reason, they are similar to each other in terms of chemical composition. These rocks have the same geological origin. However, they are quite different rocks in terms of petrographic and physical properties. For example, the CS of these three rocks is 138, 96, and 19 MPa, respectively. The 28-day CS of the concretes produced with these rocks are 42.1, 37.6, and 24.8 MPa, respectively. This is an indication that the petrographic structure and grain strength of the concrete are effective, not the chemical content or geological origin of the aggregate. The triple comparison made here shows that the strength of concrete will increase with the increase of aggregate strength. The mentioned rocks are of igneous origin and igneous rocks have similar fracture properties due to their homogeneous structures.

The comparison made for aggregates derived from igneous rocks can also be made for the carbonate rocks Limestone, Travertine, and Onyx. These rocks, which have very similar chemical properties with over 90% CaO content, are also similar in terms of geological origin, that is, they are sedimentary rocks. While the compressive strength values of these rocks are 108, 77, and 22 MPa, respectively, the 28-day CS values of the concrete produced with the aggregates of these rocks are 33.4,

42.6, and 29.6 MPa, respectively. The prominent parameter in this comparison is porosity and surface roughness rather than grain strength. It is seen that the concrete produced with Limestone, which has higher strength than travertine, has lower strength. It is seen that the porous grain structure of travertine aggregates provides a higher degree of interlocking with the mortar. Limestone in micritic structure has very few pores and aggregate surfaces are smoother than travertine. It is not possible to talk about a complete interlocking between the aggregate particles and the mortar.

CS_R of the M_8 -Micritic Limestone (108 MPa) is approximately 2 times that of the M_{15} -Dacite (65 MPa). The compressive strength of the concretes produced with these aggregates is equal. The main reason for this is the conchoidal breakage of the M_8 -aggregate and the smoothness of these fractured surfaces. Since there is not enough adherence between the cement paste and the aggregate surface, failure occurs at this interface. In this case, the grain strength alone is not enough. Crushed stone, which can develop a greater mechanical bond with cement paste due to its angular structure and rough surface, provides higher strength than gravel.

M_{12} -Claystone and M_{13} -Breccia have the same compressive strength. However, the concrete produced with M_{13} has one and a half times the strength of the concrete produced with M_{12} . In this comparison, the subject to be emphasized is the formation of aggregates, namely their structure and texture. The claystone studied in this study is the bedrock of the coal and has a laminated structure consisting of many thin layers. It is natural due to its structure to show high strength in the pressure test performed on core samples taken perpendicular to the stratification. However, when the same claystone is subjected to repeated impact movements in a jaw crusher, the layers are separated and abundant flat/long aggregate grains are formed. The grain shape of M_{13} -Breccia aggregates is more cubic. The failure of the concrete produced by Claystone is due to the weak shear strength of the coarse aggregates (thin and long).

It is noteworthy that the rocks coded as M_1 , M_2 , and M_3 have a rock strength of around 200 MPa. Although the aggregates produced from these rocks have very high grain strength, the compressive strength values obtained from the concretes in which they are used are not by far higher than the compressive strength values of the concretes produced with other aggregates. Since the water-cement ratio was kept high in this study, the full potential of the coarse aggregate was not revealed. In the mechanical tests of concrete, failure occurred mostly in cement paste or at the aggregate-mortar interface. With the ideal water-cement ratio and the use of standard fine aggregate, the strength of the mortar and aggregate in the concrete can be harmonized. In this way, the relationship between the concrete compressive strength and the rock (aggregate) compressive strength will follow a more linear course.

CS of the aggregate rocks was determined on the core specimens, which may contain some micro-cracks and fissures. However, the aggregate particles were primarily separated from these discontinuities during the crushing. Comparing the rock core specimens with the aggregate particles, the aggregate particles have little or none of the discontinuities, which causes them to be getting into a steadier structure. Therefore, each aggregate particle might have a somewhat higher strength than its corresponding rock. For new researchers who will work on this subject, it may be a more accurate approach to use the "ACV" experiment, which is an indicator of the resistance of aggregates to crushing under constant load, instead of CS_R in correlation studies.

High-strength concrete is usually made with a w/c of less than 0.4. When the strength of the mortar and the strength of the bond at the interface reach a level similar to the strength of the coarse aggregate, it may be possible to take advantage of the full potential of the coarse aggregate particles (Wu et al., 2001). It is known that if the w/c in concrete mixtures is in the range of 0.5-0.7, the coarse aggregate strength loses its importance because the mortar-aggregate bond or hydrated cement paste breaks down much earlier than aggregates (Aitcin, Sarkar & Laplante, 1990). It is seen that the full potential of coarse aggregate strength can be used in concrete mixtures where the aggregate strength is lower or close to the mortar strength (M_{16} - M_{20}). The use of crushed stone-sand in high proportion in the concrete mixtures in this study, therefore, working with a high w/c kept the effect of coarse aggregate on concrete properties at a limited level. Despite the mentioned handicaps, the equations obtained in this study revealed that hardened concrete properties can be predicted strongly by coarse aggregate properties at the end of the 28-day curing period.

In simple regression analysis, it is seen that the coefficient of determination obtained by the hardness test (SHH) is relatively low compared to the coefficient of determination determined for other parameters. The most important reason for this is that the mortar is more dominant than the aggregate on the limited surface of the concrete where the measurement is made. In all mechanical and physical tests, all cross-sections of the samples are used to affect the test result, while the surface properties of the sample are mostly effective in the hardness test.

In this study, crushed stone sand was preferred instead of river sand in order to reveal the effect of aggregate properties on concrete properties. This situation caused an increase in the w/c ratio and a relative decrease in the coarse aggregate effect. By increasing the coarse aggregate ratio and using river sand instead of crushed stone sand, it will be possible to more strongly demonstrate the effect of coarse aggregate properties on concrete properties.

For concrete strength, properties such as grain shape and porosity are just as critical as aggregate strength. Multiple regression models were constructed based on estimating dependent variables (CS_C , STS_C , LA_C , and IE_C) with four different independent variables. The most important advantage here is that all independent variables (except the 1st independent variable) in the models were selected from non-destructive testing methods (SHH, UPV, UW, Pg, and, WA). All of these tests can be applied without damaging the samples by using samples prepared for the compressive strength of rock or concrete. The fact that there is no need for additional samples shows that these multiple models can be used easily.

In the selection of the strongest multiple regression models, not only the R^2 value was taken into account, but a performance index developed by the author was used to create an accurate selection criterion. According to this criterion, the equations with the highest predictive power for CS_C , STS_C , LA_C , and IE_C were determined as Equation 15, Equation 18, Equation 22, and Equation 31, respectively.

Another finding that can be derived from the multiple regression equations is as follows. According to the mean PI_{at} values, while the equations with the highest predictive power were obtained for the STS_C (2.35), LA_C (2.28), and CS_C (2.16) properties, respectively, the equations with the weakest predictive power were determined for the IE_C (1.05) property.

Author contributions: The author confirms contribution to the paper as follows: Conceptualization, data curation, formal analysis, investigation, methodology, project administration, resources, software, supervision, validation, visualization, writing - original draft; writing - review & editing: Ahmet Teymen.

Funding: None

Acknowledgments: The author received no financial support for this research, authorship, and/or publication of this article.

Conflicts of interest: The author declares that there are no conflicts of interest.

References

- Abdullahi, M. (2012). Effect of aggregate type on compressive strength of concrete. *International Journal for Computational Civil and Structural Engineering*, 2(3), 782. <https://doi.org/10.6088/ijcser.00202030008>
- ACI Committee 221 (2001). *Guide for use of normal weight aggregate in concrete*, ACI manual of concrete practice: Part 1. Farmington Hills (MI).
- ACI Committee 544.2R-89 (Reapproved 2009). *Measurement of Properties of Fiber Reinforced Concrete*, Reported by ACI Committee 544, Farmington Hills, Michigan: American Concrete Institute.
- Ahmad, S., & Alghamdi, A. (2012). A study on effect of coarse aggregate type on concrete performance. *Arabian Journal for Science and Engineering*, 37(7), 1777-1786. <https://doi.org/10.1007/s13369-012-0282-6>
- Aitcin, P.C., & Mehda, P.K. (1990). Effect of coarse aggregate characteristics on mechanical properties of high strength concrete. *ACI Materials Journal*, 87(2), 103-107.
- Aitcin, P.C., Sarkar, S.L., & Laplante, P. (1990). Long-term characteristics of a very high strength concrete. *Concrete International*, 12(1): 40-44.

- Al-Oraimi, S.K., Taha, R., & Hassan, H.F. (2006). The effect of the mineralogy of coarse aggregate on the mechanical properties of high-strength concrete. *Construction and Building Materials*, 20, 499–503. <http://doi.org/10.1016/j.conbuildmat.2004.12.005>
- Alexander, M.G. (1993). Two experimental techniques for studying the effects of the interfacial zone between cement paste and rock. *Cement and Concrete Research*, 23(3), 567–575. [http://doi.org/10.1016/0008-8846\(93\)90006-U](http://doi.org/10.1016/0008-8846(93)90006-U)
- Alqarni, A. S., Albidah, A. S., Alaskar, A. M., & Abadel, A. A. (2020). The effect of coarse aggregate characteristics on the shear behavior of reinforced concrete slender beams. *Construction and Building Materials*, 264, 120189. <https://doi.org/10.1016/j.conbuildmat.2020.120189>
- Aminur, M.R., Harunur, M.R., Teo, D.C.L., & Abu Zakir, M.M. (2010). Effect of aggregates and curing conditions on the compressive strength of concrete with age. *Journal of Civil Engineering Science and Technology*, 1(2), 1-6. <https://doi.org/10.33736/jcest.71.2010>
- ASTM C-131-01 (2006). Resistance to degradation of small-size coarse aggregate by abrasion and impact in the Los Angeles Machine. ASTM Designation. Philadelphia: American Society for Testing Materials.
- Balaji, M., Sharma, S.D., Vigneshwaran, A., & Fayaz Ahamed, K. (2017). Experimental study on the behavior of self-compacting self-cured concrete using chemical admixtures and metakaolin; International Conference on Emerging trends in Engineering, Science and sustainable technology, (ICETSST 2017) 18-25.
- Bentz, D. P., Arnold, J., Boisclair, M. J., Jones, S. Z., Rothfeld, P., Stutzman, P. E., ... & Ardani, A. (2017). Influence of aggregate characteristics on concrete performance (No. NIST Technical Note 1963). US Department of Commerce, National Institute of Standards and Technology. <https://doi.org/10.6028/NIST.TN.1963>
- Beushausen, H., & Dittmer, T. (2015). The influence of aggregate type on the strength and elastic modulus of high strength concrete. *Construction and Building Materials*, 74, 132-139. <http://dx.doi.org/10.1016/j.conbuildmat.2014.08.055>
- Beshr, H., Almusallam, A.A., & Maslehuddin, M. (2003). Effect of coarse aggregate quality on the mechanical properties of high strength concrete. *Construction and Building Materials*, 17, 97-103. [https://doi.org/10.1016/S0950-0618\(02\)00097-1](https://doi.org/10.1016/S0950-0618(02)00097-1)
- Chi, J.M., Huang, R., Yang, C.C., & Chang, J.J. (2003). Effect of aggregate properties on the strength and stiffness of lightweight concrete. *Cement and Concrete Composites*, 25(2), 197-205. [https://doi.org/10.1016/S0958-9465\(02\)00020-3](https://doi.org/10.1016/S0958-9465(02)00020-3)
- Choi, S. (1978). *Introductory Statistics in Science*. New Jersey: Prentice-Hall Inc.
- Ćosić, K., Korat, L., Ducman, V., & Netinger, I. (2015). Influence of aggregate type and size on properties of pervious concrete. *Construction and Building Materials*, 78, 69-76. <https://doi.org/10.1016/j.conbuildmat.2014.12.073>
- de Larrard, F., & Belloc, A. (1997). The Influence of aggregate on the compressive strength of normal and high-strength concrete. *ACI Materials Journal*, 94(5), 417-426.
- Dong, J., Li, Z.Q., Yan, X., Liu, Y., Zhao, S.R., Qian, R., Zheng, Y., & Jiang, T. (2022). Effects of coarse aggregates on the mechanical properties, durability and microscopic behaviour of mortar rubble. *Construction and Building Materials*, 354, 129187. <https://doi.org/10.1016/j.conbuildmat.2022.129187>
- Ezeldin, A.S., & Aitcin, P.C. (1991). Effects of coarse aggregate on the behaviour of normal and high strength concretes. *Cement Concrete and Aggregates*, 13(2), 121-124. <https://doi.org/10.1520/CCA10128J>
- French, C.W., & Mokhtarzadeh, A. (1993). High strength concrete: effects of materials, curing and test procedures on short-term compressive strength. *PCI Journal*, 38(3), 76-87.
- Góra, J., & Piasta, W. (2020). Impact of mechanical resistance of aggregate on properties of concrete. *Case Studies in Construction Materials*, 13, e00438. <https://doi.org/10.1016/j.cscm.2020.e00438>
- Góra, J., & Szafraniec, M. (2020). Influence of maximum aggregate grain size on the strength properties and modulus of elasticity of concrete. *Applied Sciences*, 10(11), 3918. <https://doi.org/10.3390/app10113918>
- Hansen, B. S., Carey, A. S., & Howard, I. L. (2021). Effects of aggregate shape and mineralogy on relationships between concrete mechanical properties. *ACI Materials Journal*, 118(5), 115-124. <http://doi.org/10.14359/51732933>
- Hussin, A., & Poole, C. (2011). Petrography evidence of the interfacial transition zone (ITZ) in the normal strength concrete containing granitic and limestone aggregates. *Construction and Building Materials*, 25, 2298-2303. <http://doi.org/10.1016/j.conbuildmat.2010.11.023>
- Hong, L., Gu, X.L., & Lin, F. (2014). Influence of aggregate surface roughness on mechanical properties of interface and concrete. *Construction and Building Materials*, 65, 338–349. <http://doi.org/10.1016/j.conbuildmat.2014.04.131>
- <https://www.statista.com/statistics/219343/cement-production-worldwide/>
- ISRM (2007). The complete ISRM suggested methods for rock characterization, testing and monitoring: 1974–2006. Suggested methods prepared by the commission on testing methods, international society for rock mechanics. In: Ulusay R, Hudson JA (eds) *Compilation arranged by the ISRM Turkish national group*, Ankara, Turkey, Kozan Ofset.
- Kamali-Bernard, S., Keinde, D., & Bernard, F. (2014). Effect of aggregate type on the concrete matrix/aggregates interface and its influence on the overall mechanical behavior. A numerical study. *Key Engineering Materials*, 617, 14-17. <http://doi.org/10.4028/www.scientific.net/KEM.617.14>

- Karaman, K., & Bakhytzhan, A. (2020). Prediction of concrete strength from rock properties at the preliminary design stage. *Geomechanics and Engineering*, 23(2), 115-125, <https://doi.org/10.12989/gae.2020.23.2.115>
- Kılıç, A., Atiş, C.D., Teymen, A., Karahan, O., Özcan, F., Bilim, C., & Özdemir, M. (2008). The influence of aggregate type on the strength and abrasion resistance of high strength concrete. *Cement and Concrete Composites*, 30, 290-296. <https://doi.org/10.1016/j.cemconcomp.2007.05.011>
- Kılıç, A., & Sertabipoğlu, Z. (2015). Effect of heat treatment on pozzolanic activity of volcanic pumice used as cementitious material. *Cement and Concrete Composites*, 57, 128-132. <https://doi.org/10.1016/j.cemconcomp.2014.12.006>
- Kılıç, A., Teymen, A., Özdemir, O., & Atiş, C.D. (2019). Estimation of compressive strength of concrete using physico-mechanical properties of aggregate rock. *Iranian Journal of Science and Technology, Transactions of Civil Engineering*, 43, 171-178. <https://doi.org/10.1007/s40996-018-0156-6>.
- Liu, Y., & Presuel-Moreno, F. (2014). Effect of elevated temperature curing on compressive strength and electrical resistivity of concrete with fly ash and ground-granulated blast-furnace slag. *ACI Materials Journal*, 111(5), 531-541.
- Mannan, M.A., Basri, H.B., Zain, M.F.M., & Islam, M.N. (2002). Effect of curing conditions on the properties of OPS-concrete. *Building and Environment*, 37:1167-1171. [https://doi.org/10.1016/S0360-1323\(01\)00078-6](https://doi.org/10.1016/S0360-1323(01)00078-6)
- Meddah, M.S., Zitouni, S., & Belâabes, S. (2010). Effect of content and particle size distribution of coarse aggregate on the compressive strength of concrete. *Construction and Building Materials*, 24(4), 505-512. <https://doi.org/10.1016/j.conbuildmat.2009.10.009>
- Miller, C., Vasconcelos, K., Little, D., & Bhasin, A. (2011). Investigating aspects of aggregate properties that influence asphalt mixtures performance. Research Report for DTFH61-06-C-00021, Texas A&M University at College Station and the University of Texas at Austin, Texas.
- Miskovsky, K., Tabora, D.M., Kou, S.Q., & Lindqvist, P.A. (2004). Influence of the mineralogical composition and textural properties on the quality of coarse aggregates. *Journal of Materials Engineering and Performance*, 13, 144-150. <http://doi.org/10.1361/10599490418334>
- Monteiro, P.J.M., & Mehta, P.K. (1986). Interaction between carbonate rock and cement paste. *Cement and Concrete Research*, 16(2), 127-134. [http://doi.org/10.1016/0008-8846\(86\)90128-6](http://doi.org/10.1016/0008-8846(86)90128-6)
- Mostofinejad, D., Bahmani, H., Eshaghi-Milasi, S., & Nozhati, M. (2023). Empirical relationships for prediction of mechanical properties of high-strength concrete. *Iranian Journal of Science and Technology, Transactions of Civil Engineering*, 47(1), 315-332. <https://doi.org/10.1007/s40996-022-01023-4>
- Mousavi, S. M., & Ranjbar, M. M. (2021). Experimental study of the effect of silica fume and coarse aggregate type on the fracture characteristics of high-strength concrete. *Engineering Fracture Mechanics*, 258, 108094. <https://doi.org/10.1016/j.engfracmech.2021.108094>
- Naderi, M., & Kaboudan, A. (2021). Experimental study of the effect of aggregate type on concrete strength and permeability. *Journal of Building Engineering*, 37, 101928. <https://doi.org/10.1016/j.job.2020.101928>
- Neville, A.M. (1981). *Properties of Concrete*. 3rd Ed., Longman Scientific, London, 287.
- Neville, A.M. (1995). *Properties of concrete*. 4th ed. London: Longman Group UK Limited Press.
- Özturan, T., & Çeçen, C. (1997). Effect of coarse aggregate type on mechanical properties of concretes with different strengths. *Cement and Concrete Research*, 27(2), 165-170. [https://doi.org/10.1016/S0008-8846\(97\)00006-9](https://doi.org/10.1016/S0008-8846(97)00006-9)
- Patowary, F., & Al Mahmood, R. (2022). Effect of local coarse aggregate type on concrete mechanical properties in Bangladesh. *International Journal of Engineering and Advanced Technology*, 11(4). <http://doi.org/10.35940/ijeat.D3490.0411422>
- Petrounias, P., Rogkala, A., Kalpogiannaki, M., Tsikouras, B., & Hatzipanagiotou, K. (2016). Comparative study of physico-mechanical properties of ultra-basic rocks and andesites from central Macedonia (Greece). *Bulletin of the Geological Society of Greece*, 50(4), 1989-1998. <http://doi.org/10.12681/bgsg.11945>
- Petrounias, P., Giannakopoulou, P.P., Rogkala, A., Stamatis, P.M., Tsikouras, B., Papoulis, D., Lampropoulou, P., & Hatzipanagiotou, K. (2018a). The influence of alteration of aggregates on the quality of the concrete: A case study from serpentinites and andesites from central Macedonia (North Greece). *Geosciences Journal*, 8(4), 115. <https://doi.org/10.3390/geosciences8040115>
- Petrounias, P., Giannakopoulou, P.P., Rogkala, A., Lampropoulou, P., Koutsopoulou, E., Papoulis, D., Tsikouras, B., & Hatzipanagiotou, K. (2018b). The impact of secondary phyllosilicate minerals on the engineering properties of various igneous aggregates from Greece. *Minerals*, 8(8), 329. <http://doi.org/10.3390/min8080329>
- Qudoos, A., Rehman, A., Kim, H.G., & Ryou, J.S. (2018). Influence of the surface roughness of crushed natural aggregates on the microhardness of the interfacial transition zone of concrete with mineral admixtures and polymer latex. *Construction and Building Materials*, (168), 946-957. <http://doi.org/10.1016/j.conbuildmat.2018.02.205>
- Quiroga, P.N., & Fowler, D.W. (2003). The effects of aggregates characteristics on the performance of Portland cement concrete. *International Centre for Aggregate Research*, ICAR 104-1F.
- Rigopoulos, I., Tsikouras, B., Pomonis, P., & Hatzipanagiotou, K. (2010). The influence of alteration on the Engineering properties of dolerites: The example from the Pindos and Vourinos ophiolites (northern Greece). *International Journal of Rock Mechanics and Mining Sciences*, 47(1), 69-80. <http://doi.org/10.1016/j.ijrmms.2009.04.003>

- Rocco, C., & Elices, M. (2008). Effect of aggregate shape on the mechanical properties of a simple concrete. *Engineering Fracture Mechanics*, 76(2), 286-298. <http://doi.org/10.1016/j.engfracmech.2008.10.010>
- SPSS Inc. SPSS regression models (version 17.0). Available from: (<http://www.spss.com>)
- TS EN 706 12620+A1 (2009). Aggregates for concretes. Turkish Standard Institution, Ankara.
- TS EN-197-1 (2004). Cements-part 1: Compositions and conformity criteria for common cements. Turkish Standards Institute, TSE, Turkey.
- TS EN 12390-3:2009/AC (2012). Testing hardened concrete- part 3: compressive strength of test specimens. Ankara: Turkish Standard Institution.
- TS EN 12390-6 (2010). Testing Hardened Concrete – Part 6: Tensile Splitting Strength of Test Specimens, Turkish Standards Institute, TSE, Turkey.
- TS EN 12407 (2013). Natural Stone Test Methods – Petrographic Examination, Institute of Turkish Standards, 17.
- TS EN 12504-4 (2012). Testing concrete- part 4: determination of ultrasonic pulse velocity. Ankara: Turkish Standard Institution.
- TS EN 934-2 (2011). Admixtures for concrete, mortar and grout-part 2: concrete admixtures-definitions, requirements, conformity marking and labeling. Turkish Standards Institute, TSE, Turkey.
- Teymen, A., & Mengüç, E.C. (2020). Comparative evaluation of different statistical tools for the prediction of uniaxial compressive strength of rocks. *International Journal of Mining Science and Technology*, 30(6), 785-797. <https://doi.org/10.1016/j.ijmst.2020.06.008>.
- Tiryaki, B. (2008). Application of artificial neural networks for predicting the cuttability of rocks by drag tools. *Tunnelling and Underground Space Technology*, 23(3), 273-280. <https://doi.org/10.1016/j.tust.2007.04.008>
- Tugrul, A., & Zarif, I.H. (1999). Correlation of mineralogical and textural characteristics with engineering properties of selected granitic rocks from Turkey. *Engineering Geology*, 51(4), 303–317. [http://doi.org/10.1016/S0013-7952\(98\)00071-4](http://doi.org/10.1016/S0013-7952(98)00071-4)
- Tunc, E.T., & Alyamac, K.E. (2020). Determination of the relationship between the Los Angeles abrasion values of aggregates and concrete strength using the Response Surface Methodology. *Construction and Building Materials*, 260, 119850. <https://doi.org/10.1016/j.conbuildmat.2020.119850>
- Uysal, M. (2012). The influence of coarse aggregate type on mechanical properties of fly ash additive self-compacting concrete. *Construction and Building Materials*, 37, 533-540. <http://dx.doi.org/10.1016/j.conbuildmat.2012.07.085>
- Vishalakshi, K.P., Revathi, V., & Reddy, S.S. (2018). Effect of type of coarse aggregate on the strength properties and fracture energy of normal and high strength concrete. *Engineering Fracture Mechanics*, 194, 52-60. <https://doi.org/10.1016/j.engfracmech.2018.02.029>
- Wang, L., Yong, H., Lu, J., Shu, C., & Wang, H. (2021). Influence of coarse aggregate type on the mechanical strengths and durability of cement concrete. *Coatings*, 11(9), 1036. <https://doi.org/10.3390/coatings11091036>
- Wu, K.R., Chen, B., Yao, W., & Zhang, D. (2001). Effect of coarse aggregate type on mechanical properties of high-performance concrete. *Cement and Concrete Research*, 3, 1421-1425. [https://doi.org/10.1016/S0008-8846\(01\)00588-9](https://doi.org/10.1016/S0008-8846(01)00588-9)
- Wu, F., Xu, L., Chi, Y., Zeng, Y., Deng, F., & Chen, Q. (2020). Compressive and flexural properties of ultra-high performance fiber-reinforced cementitious composite: The effect of coarse aggregate. *Composite Structures*, 236, 111810. <https://doi.org/10.1016/j.compstruct.2019.111810>
- Xing, Z., Beacour, A.L., Hebert, R., Noumowe, A., & Ledesert, B. (2015). Aggregate's influence on thermophysical concrete properties at elevated temperature. *Construction and Building Materials*, 95, 18-28. <https://doi.org/10.1016/j.conbuildmat.2015.07.060>
- Yehia, S., Abdelfatah, A., & Mansour, D. (2020). Effect of aggregate type and specimen configuration on concrete compressive strength. *Crystals*, 10(7), 625. <https://doi.org/10.3390/cryst10070625>
- Yılmaz, N.G., Goktan, R.M., & Kibici, Y. (2011). Relations between some quantitative petrographic characteristics and mechanical strength properties of granitic building stones. *International Journal of Rock Mechanics and Mining Sciences*, 48, 506–513. <http://doi.org/10.1016/j.ijrmms.2010.09.003>
- Yılmaz, M., & Tuğrul, A. (2012). The effects of different sandstone aggregates on concrete strength. *Construction and Building Materials*, 35, 294-303. <https://doi.org/10.1016/j.conbuildmat.2012.04.014>
- Zhang, M., & Gjorv, O.E. (1990). Microstructure of the interfacial zone between lightweight aggregate and cement paste. *Cement and Concrete Research*, 20(4), 610–618. [http://doi.org/10.1016/0008-8846\(90\)90103-5](http://doi.org/10.1016/0008-8846(90)90103-5)
- Zhou, F.P., Lydon, F.D., & Barr, B.I.G. (1995). Effect of coarse aggregate on elastic modulus and compressive strength of high performance concrete. *Cement and Concrete Research*, 25(1), 177-186. [https://doi.org/10.1016/0008-8846\(94\)00125-1](https://doi.org/10.1016/0008-8846(94)00125-1)
- Zunino, F., Castro, J., & Lopez, M. (2015). Thermo-mechanical assessment of concrete microcracking damage due to early-age temperature rise. *Construction and Building Materials*, 81, 140–153. <http://doi.org/10.1016/j.conbuildmat.2014.12.126>



Copyright (c) 2023 Teymen, A. This work is licensed under a [Creative Commons Attribution-Noncommercial-No Derivatives 4.0 International License](https://creativecommons.org/licenses/by-nc-nd/4.0/).